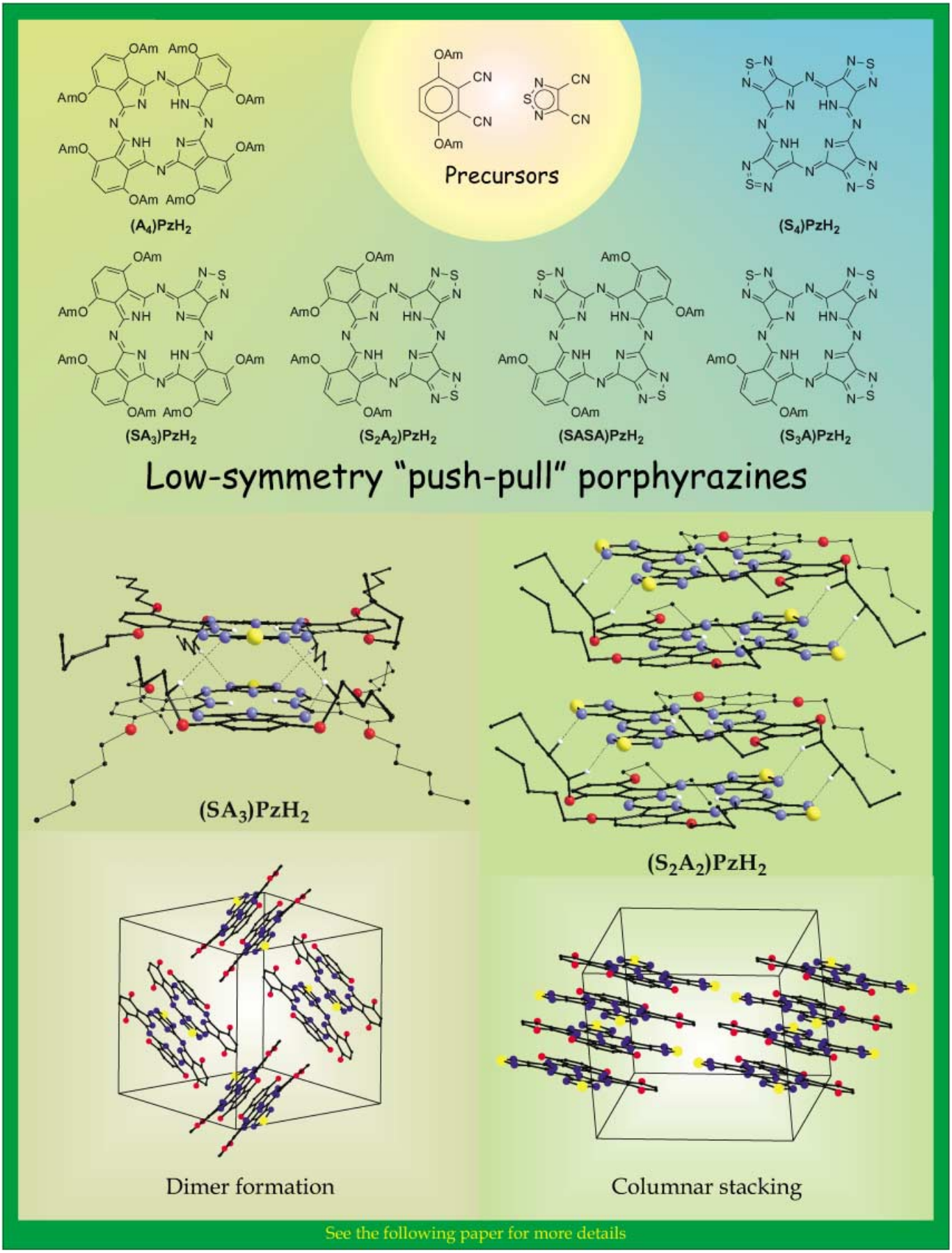


 DOI: 10.1002/chem.200304929  

# Synthesis, X-ray Crystal Structure, UV/Visible Linear and Nonlinear (Optical Limiting) Spectral Properties of Symmetrical and Unsymmetrical Porphyrazines with Annulated 1,2,5-Thiadiazole and 1,4-Diamyloxybenzene Moieties

**Maria Pia Donzello,[a] Claudio Ercolani,*[a] Anna A. Gaberkorn,[b] Evgenij V. Kudrik,[b] Moreno Meneghetti,[c] Gabriele Marcolongo,[c] Corrado Rizzoli,[d] and Pavel A. Stuzhin*[b]**

**Abstract:** Co-cyclization of 1,2,5-thiadiazole-3,4-dicarbonitrile and 3,6-diamyloxyphthalodinitrile in the presence of magnesium or lithium amylate in amyl alcohol leads to mixtures containing the Mg derivatives of the symmetrical species tetrakis(1,2,5-thiadiazolo)porphyrazine, $(S_4)PzH_2$, and tetrakis(1,4-diamyloxybenzo)porphyrazine, $(A_4)PzH_2$, and the low-symmetry macrocycles bearing peripheral 1,2,5-thiadiazole and 1,4-diamyloxybenzene rings in the ratio 1:3, 2:2 (*cis* and *trans*), and 3:1, that is, $(SA_3)PzH_2$, $(S_2A_2)PzH_2$, $(SASA)PzH_2$, and $(S_3A)PzH_2$, respectively. The basic Mg materials were converted to the corresponding free-base macrocycles by treatment with $CF_3COOH$. The species were separated from the mixtures by chromatography, either as Mg complexes or demetalated materials. With results on $(S_4)PzH_2$ and $(SA_3)PzH_2$ in hand, including crystallographic work on the latter, a general chemical physical investigation has been carried out of all the symmetrical and unsymmetrical free-base macrocycles. The structures of the species $(S_2A_2)PzH_2$ and $(A_4)PzH_2$. were elucidated by single-crystal X-ray crystallography. The effect of the progressive variation of the macrocyclic structure along the series, from the symmetrical $(S_4)PzH_2$ to its symmetrical partner $(A_4)PzH_2$ via the low-symmetry 3:1, 2:2 (*cis* and *trans*), and 1:3 macrocycles, was studied by IR, $^1H$ NMR, and UV/Vis linear and nonlinear (optical limiting) measurements. The results are interpreted on the basis of intra- and intermolecular interactions between the electron-deficient 1,2,5-thiadiazole and the electron-donating 1,4-diamyloxybenzene moieties.

**Keywords:** nonlinear optics · porphyrazines · sulfur heterocycles · solvatochromism · structure elucidation

## Introduction

The free-ligand phthalocyanine macrocycle, its metal derivatives, and the peripherally symmetrically substituted analogues form the most widely extended class of porphyrazine systems which are currently under intensive investigation both in terms of basic research and for a number of applications.[1, 2] Recently, we reported new types of symmetrical tetrapyrrolic phthalocyanine-like macrocycles, namely, tetrakis(1,2,5-thiadiazole)porphyrazines, [TTDPzM],[3, 4] and their Se analogues, [TSeDPzM],[5, 6] (M = Mg, 2H, and bivalent first transition series metals, Scheme 1), that contain five-membered electron-deficient heterocycles annulated on

[a] Prof. C. Ercolani, Dr. M. P. Donzello
Dipartimento di Chimica, Università degli Studi di Roma "La Sapienza"
P.le A. Moro 5, 00185 Roma (Italy)
Fax: (+39) 6-49913332
E-mail: claudio.ercolani@uniroma1.it

[b] Doz. Dr. P. A. Stuzhin, A. A. Gaberkorn, Dr. E. V. Kudrik
Department of Organic Chemistry
Ivanovo State University of Chemical Technology
Friedrich Engels Pr-t 7, 153460 Ivanovo (Russian Federation)
Fax: (+7) 0932-374897
E-mail: stuzhin@isuct.ru

[c] Prof. M. Meneghetti, Dr. G. Marcolongo
Dipartimento di Chimica Fisica, Università di Padova
Via Loredan 2, 35131 Padova (Italy)

[d] Prof. C. Rizzoli
Dipartimento di Chimica Generale ed Inorganica, Università di Parma
Viale delle Scienze, 43100 Parma (Italy)

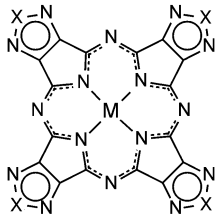


Scheme 1. Schematic representation of a tetrakis(thia(seleno)diazolo)porphyrazine macrocycle (M = Mg, $H_2$, bivalent first transition series metal ions).



DOI: 10.1002/chem.200304929

the pairs of $C_\beta$ atoms of the inner pyrrole rings. Common to these new classes of porphyrazines and their phthalocyanine analogues are a number of features and properties, such as π-electron delocalization extended throughout the macrocycle, high chromophoricity, and associated solution UV/Vis spectral behavior, thermal stability, low solubility, sublimability (as to the sulfur-containing species).

In connection with, and in extension of this work, efforts have recently been successfully directed towards the synthesis of a new series of low-symmetry porphyrazines that bear peripheral annulated 1,2,5-thiadiazole (or 1,2,5-selenodiazole) and 1,4-diamyloxybenzene rings. As anticipated,[7] all members of the series of the unmetalated low-symmetry species shown in Scheme 2, that is, the 1:3 $(SA_3)PzH_2$, the 2:2 *cis* and *trans* species $(S_2A_2)PzH_2$ and $(SASA)PzH_2$, and the 3:1 $(S_3A)PzH_2$, have been isolated (A symbolizes the annulated 1,4-diamyloxybenzene ring and S the 1,2,5-thiadiazole ring in the pertinent fragments of the porphyrazine macrocycle). The individual species were characterized with differing degrees of accuracy. Attention was also given to the corresponding symmetrical octaamyloxy-substituted phthalocyanine, $(AmO)_8PcH_2$, denoted here as $(A_4)PzH_2$ (Scheme 2). The tetrakis(1,2,5-thiadiazolo)porphyrazine, $(S_4)PzH_2$ (previously used abbreviation: $TTDPzH_2$[3, 4]), completes the series. Recently, the synthetic aspects, X-ray structural elucidation, and UV/Vis spectral properties of the 1:3 species $(SA_3)PzH_2$ and its Se analogue $(SeA_3)PzH_2$ were briefly reported.[8, 9] A detailed picture of the new information now available on the synthesis, X-ray structural work, and IR, $^1$H NMR, and UV/Vis spectral behavior of the species shown in Scheme 2 is given here. The present series of macrocycles is one of the few sets of unsymmetrical and related symmetrical metal-free porphyrazine materials isolated so far and also characterized by single-crystal X-ray diffraction,[10] and, indeed, an exclusive representative set in the field of porphyrazine macrocycles carrying annulated heteroaromatic rings.[11]

It is well-known that the prospects for applications in nonlinear optics is a relevant research topic for phthalocyanine systems.[12–16] These molecular structures have been shown to be interesting for applications such as optical limiting of ns pulses because of the strong excited-state absorption of their triplet states. Noticeably, the examination of the optical limiting effect (related to the third or higher order responses) for a series of strictly related symmetrical and unsymmetrical porphyrazines can be a worthwhile effort. Indeed, low-symmetry "push–pull" porphyrazines are promising materials for second-order nonlinear optics,[13, 17] and the number of unsymmetrical porphyrazines carrying, in addition to benzene rings, π-acceptor or π-donor heterocycles annulated directly to the central tetrapyrrolic macrocycle (that is, pyrazine,[18, 19] pyridine,[20, 21] thiophene,[22, 23] imidazole,[24] and pyrrole[23]) has increased considerably recently. In view of more extended studies of nonlinear optical properties in the future, the present series of symmetrical and unsymmetrical macrocycles has been investigated for their optical limiting behavior, and the results are also illustrated below.

**Abstract in Italian:** *La cociclizzazione dell' 1,2,5-tiadiazol-3,4-dicarbonitrile e del 3,6-diamilossiftalodinitrile sotto opportune condizioni sperimentali porta alla formazione di metallocomplessi (Mg) della tetrakis(tiadiazol)porfirazina ($(S_4)PzH_2$), della tetrakis(1,4-diamilossibenzene)porfirazina ($(A_4)PzH_2$), e di specie a bassa simmetria di formule $(SA_3)PzH_2$, $(S_2A_2)PzH_2$, $(SASA)PzH_2$, e $(S_3A)PzH_2$). I complessi di $Mg^{II}$ sono convertiti nei corrispondenti leganti liberi mediante trattamento con $CF_3COOH$. La scomposizione delle miscele nelle singole specie componenti, sia come complessi di $Mg^{II}$ che come leganti liberi, è stata ottenuta con metodi cromatografici. Delle specie $(S_2A_2)PzH_2$ e $(A_4)PzH_2$ è stata risolta la struttura mediante raggi X su cristallo singolo. Per tutte le specie isolate, simmetriche ed asimmetriche, è stato condotto un approfondito studio chimico-fisico (IR, $^1$H NMR, UV/Vis, optical limiting). Una generale considerazione dei risultati ottenuti ha permesso di evidenziare il ruolo svolto dai frammenti 1,2,5-tiadiazolico e 1,4-diamilossibenzenico nel determinare le proprietà spettroscopiche e la struttura molecolare ed elettronica sia di specie simmetriche che asimmetriche.*

**Abstract in Russian:** Соконденсацией 1,2,5-тиадиазол-3,4-дикарбонитрила и 3,6-диамилоксифталодинитрила в присутствии амилатов лития или магния в амиловом спирте получена смесь металлопорфиразинов, из которой была выделена полная серия несимметрично аннелированных порфиразинов, содержащих фрагменты 1,2,5-тиадиазола (S) и 1,4-диамилоксибензола (A) в соотношении 1:3, 2:2 (цис- и транс-) и 3:1, т.е. $(SA_3)PzH_2$, $(S_2A_2)PzH_2$, $(SASA)PzH_2$, $(S_3A)PzH_2$. Спектроскопическое исследование ($^1$H ЯМР, ИК и ЭСП) этих порфиразинов и их симметричных аналогов $(S_4)PzH_2$, и $(A_4)PzH_2$, рентгено-структурный анализ $(S_2A_2)PzH_2$, $(SA_3)PzH_2$ и $(A_4)PzH_2$, а также изучение нелинейных оптических свойств (эффект лимитирования), показали существенное влияние на строение и физико-химические свойства внутри- и межмолекулярных взаимодействий между электронодефицитными 1,2,5-тиадиазольными и электронодонорными 1,4-диамилоксибензольными фрагментами.

## Results and Discussion

**Synthetic methods**: Condensation of *ortho*-dinitriles in boiling $C_3-C_5$ alcohols in the presence of the corresponding magnesium or lithium alcoholates is a standard method for the preparation of phthalocyanines and other porphyrazines (Linstead's method).[25, 26] Similarly, unsymmetrical phthalocyanines and porphyrazines can be prepared by co-cyclization of two different *ortho*-dinitriles. We have used this approach for the synthesis of the unsymmetrical porphyrazines shown in Scheme 2, obtained by demetalation of the corresponding Li or Mg derivatives. As is briefly illustrated here below (see the Experimental Section for more details), a number of reaction attempts under different experimental conditions and tedious purification methods were required to prepare and purify all the low-symmetry species.

*The lithium amylate method*: If the co-cyclization reaction of dinitriles **1** and **2** (Scheme 2) proceeds in the presence of lithium amylate in amyl alcohol, a mixture of the symmetrical and unsymmetrical porphyrazines **3a**–**8a** is obtained. How-

  

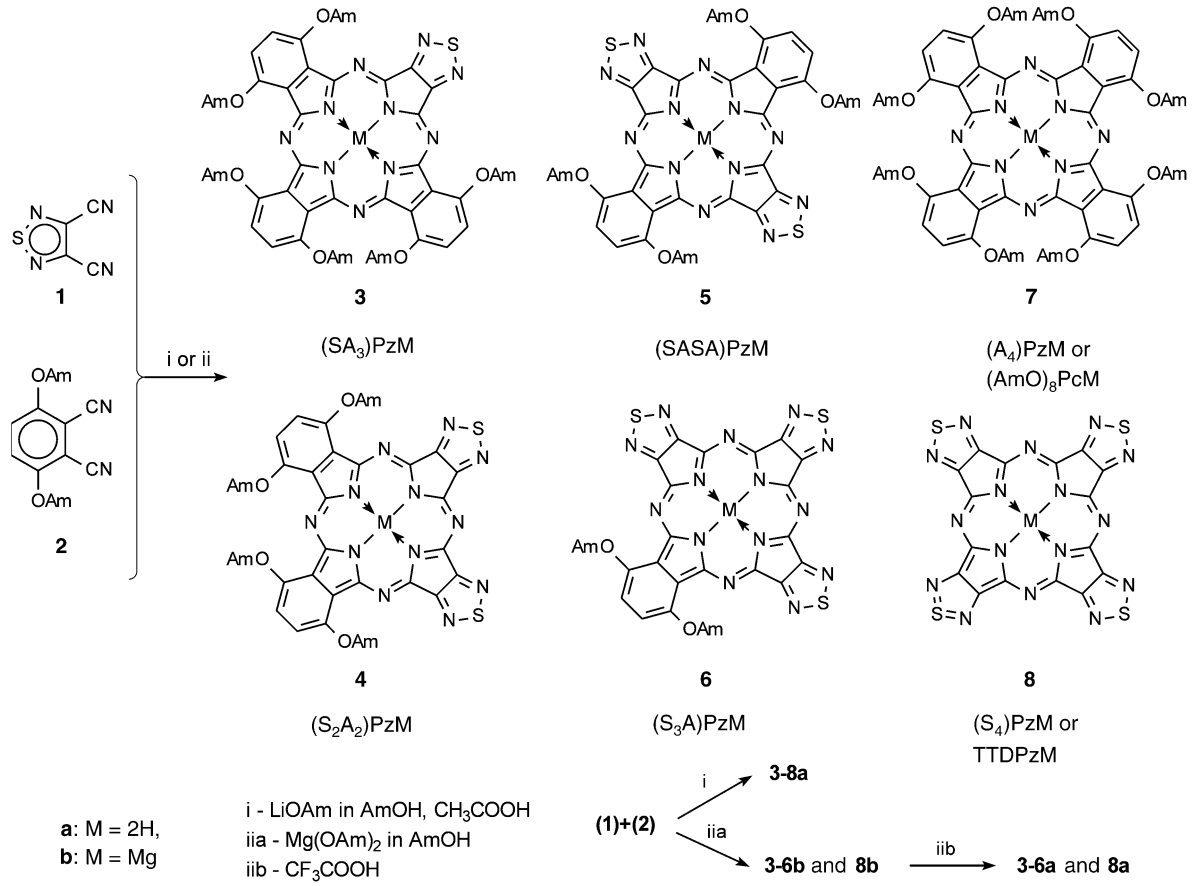


Scheme 2. Schematic representations of the precursors 1,2,5-thiadiazole-3,4-dicarbonitrile and 3,6-diamyloxyphthalodinitrile as well as their symmetrical and unsymmetrical macrocyclic derivatives.

ever, by varying the molar ratio of the two precursors **1** and **2**, it is possible, to some extent, to modify the relative amounts of the single species present in the reaction mixture. Thus, for instance, a **1**:**2** ratio in the range 1:6 – 1:10 favors the formation of the unsymmetrical porphyrazine $(SA_3)PzH_2$ (**3a**), although a considerable amount (≈30%) of the symmetrical species $(A_4)PzH_2$ (**7a**) mixed with minor amounts of all the other low-symmetry members of the series is formed. The symmetrical porphyrazine $(S_4)PzH_2$ (**8a**) is also formed in significant amounts (≈30%). This proves the high tendency of the formation of the latter despite the unfavorable **1**:**2** ratio conditions. This may be a consequence of the presence of the π-electron-deficient 1,2,5-thiadiazole rings in **1** as well as a reduction in the reactivity of **2** because of the electron-donating properties and steric hindrance effects of the amyloxy groups. In fact, both AM1 and PM3 quantum-chemical methods indicate a stronger polarization of the C≡N bonds in **1** than in **2**, and locate positive charges on the N atoms of the cyano groups in **1** (C(−0.077)≡N(+0.034) AM1 method), whereas in **2**, as well as in the unsubstituted phthalodinitrile, both N and C atoms of the CN group are negatively charged (C(−0.104)≡N(−0.019) for **2**, as obtained by AM1 method).[27] The type of polarization of the C≡N bonds in **1** is evidently more favorable with respect to the formation of intermediates of the type **9** and **10** (Scheme 3) in the cyclotetramerization reaction.

*The magnesium amylate method*: The advantage of carrying out the cross-cyclization reaction by mixing **1** and **2** in the presence of magnesium amylate is that it only provides a mixture of the 1,2,5-thiadiazole-annulated Mg-porphyrazines in the complete absence of the symmetrical octaamyloxy-substituted Mg-phthalocyanine [$(A_4)PzMg$] (**7b**). Again, however, because of the different reactivity of **1** and **2**, even using an excess of **2**, up to 30% of **1** is converted to the

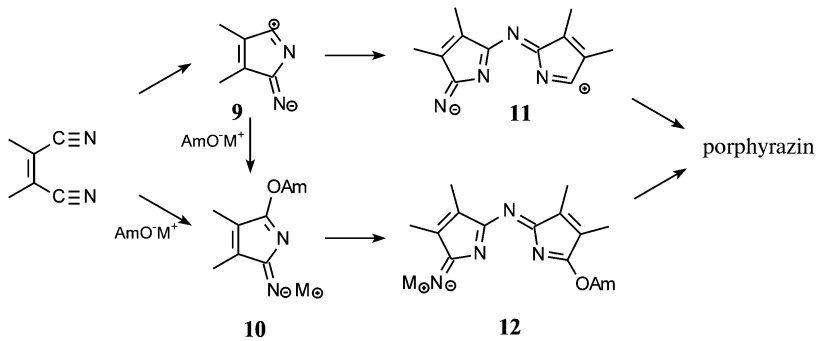


Scheme 3. Possible mechanisms for the formation of porphyrazine macrocycles.

corresponding symmetrical 1,2,5-thiadiazole-annulated Mg derivative [$(S_4)$PzMg] (**8b**). Demetalation of the mixture of the Mg species by reaction with $CF_3COOH$ allows easy conversion to the corresponding mixture of the free ligands, although with some loss of the material.

Several attempts to improve the yield of the Mg derivative of the 1:3 species $(SA_3)PzH_2$ (**3a**) were made by adding first the dinitrile **2** to the suspension of magnesium amylate in amyl alcohol and then refluxing the mixture for ≈10–15 min, thus allowing the formation of more reactive condensation intermediates of type **10** (Scheme 3; no symmetrical $Mg^{II}$ phthalocyanine **7b** was formed under these conditions). Nevertheless, when dinitrile **1** was later added, and the reaction mixture was refluxed for an additional 6–8 h, no formation of the 1:3 species **3b** was observed, whereas, instead, the relative amount of the 2:2 *cis* complex **4b** was increased. This seems to indicate that when dinitrile **2** is first refluxed with magnesium amylate, the dimeric intermediates **11**, or more likely **12** (Scheme 3), are formed. Similar dimeric intermediates have been either postulated or isolated from the synthetic reactions of phthalocyanines.[26, 28–30] Addition of the reactive dinitrile **1** to the reaction mixture containing the dimeric intermediates **11** and **12** formed from **2** leads to the Mg derivative of the *cis* isomer $(S_2A_2)PzH_2$ (**4a**). The dissociation of fragment **12** in the presence of the more reactive dinitrile **1** also resulted in the formation of the other unsymmetrical Mg-porphyrazines, although with the exclusion of [$(SA_3)$PzMg] (**3b**). Hence, this procedure is mostly favorable for the preparation of the *cis* isomeric species [$(S_2A_2)$PzMg] (**4b**), and subsequently of the corresponding free-ligand $(S_2A_2)PzH_2$ (**4a**). In view of other recent reports[30, 31] on the formation of "adjacent" (i.e. *cis*-type) phthalocyanines by use of the lithium alkoxide method, the approach involving preliminary dimerization of a less-reactive dinitrile with subsequent co-condensation with a more reactive dinitrile, seems to be generally useful for the preparation of *cis*-arranged porphyrazines.

Relatively large amounts of the corresponding 2:2 *trans*-complex are formed when dinitriles **1** and **2** (ratio 1:1–3:1) are added to the magnesium amylate suspension simultaneously. By combining **1** and **2** at a ratio of ≈5:1, the amount of the 3:1 species [$(S_3A)$PzMg] (**6b**) (Scheme 2) in the cross-cyclotetramerization was increased.

Evidently, the methodology applied for the subsequent chromatographic purification is crucial for isolation of the individual porphyrazines from their mixture. With reference to the species given in Scheme 2, owing to the insolubility of the symmetrical [$(S_4)$PzMg] (**8b**) in benzene or chloroform, separation of all the others from it is easily accomplished by Soxhlet extraction. Subsequent chromatography allows separation of the components in the solution as Mg complexes, or eventually as free ligands, after demetalation. When present in the mixture, the octaamyloxy macrocycle $(A_4)PzH_2$ (**7a**) is eluted as the first fraction with benzene on alumina. The 1:3 species $(SA_3)PzH_2$ (**3a**) is then obtained as an olive-green fraction either with benzene/chloroform (3:1) or with $CH_2Cl_2$. Elution with $CHCl_3$, or $CH_2Cl_2$ containing 1–2% MeOH, is subsequently used for the separation of the 2:2 *cis* and *trans* species, which are not easy to isolate from each other because they have very close chromatographic mobilities. No definite chromatographic procedure could be unequivocally established for the complete separation of these two isomers. When a mixture of them was eluted on alumina with $CH_2Cl_2/CHCl_3$ (1:1), a very broad green band formed along the column allowed separation of the *cis* and *trans* isomers, $(S_2A_2)PzH_2$ (**4a**) and $(SASA)PzH_2$ (**5a**), from the lower and the upper part, respectively.

The 3:1 macrocycle $(S_3A)PzH_2$ (**6a**) has very low chromatographic mobility and cannot be eluted by $CH_2Cl_2$ or $CHCl_3$, even in a mixture with considerable amounts of acetone or MeOH (≤10–30%). Very small amounts of $(S_3A)PzH_2$ could be extracted from alumina with boiling $CHCl_3$. Interestingly, pyridine or DMF, which are normally stronger eluents, appear to be completely ineffective in this case. An explanation for this is that the macrocycle is deprotoned in pyridine because of the marked acidic character of the $(S_3A)PzH_2$ species as a consequence of the presence of the three electron-withdrawing 1,2,5-thiadiazole units. Thus, a saltlike species $[(S_3A)Pz]^{2-}(pyH^+)_2$ is formed. This is similar to what happens to $(S_4)PzH_2$ in the same solvent,[3] and elution is thus prevented. An alternative solution to this problem is to work on a mixture of the related magnesium species. From a mixture of these latter complexes, chromatography on alumina of the DMF extract affords a first fraction containing the 2:2 isomers [$(S_2A_2)$PzMg] (**4b**) and [$(SASA)$PzMg] (**5b**) together with the 1:3 porphyrazine [$(SA_3)$PzMg] (**3b**). The following well-separated bluish-green fraction contains the 3:1 species [$(S_3A)$PzMg] (**6b**), whereas the symmetrical complex [$(S_4)$PzMg] (**8b**), being slightly soluble in DMF, has very low chromatographic mobility and remains as a blue band on the top of the column.

**X-ray crystallography**: Crystal data for the 2:2 *cis* isomer $(S_2A_2)PzH_2$ (9,12,14,17-tetraamyloxy-19*H*,21*H*-dibenzo[*l*,*q*]-di[1,2,5]thiadiazolo[3,4-*b*:3,4-*g*]porphyrazine) are listed in Table 1. Figure 1 shows an ORTEP top view of the macrocycle. The detailed description of the structure of the *cis*-2:2 species $(S_2A_2)PzH_2$ is presented here and compared with the structure of the 1:3 porphyrazine $(SA_3)PzH_2$, recently reported in a preliminarily communication.[8] X-ray data of the

Table 1. Experimental data for the X-ray diffraction studies on the crystalline *cis* 2:2 isomer $(S_2A_2)PzH_2$.

| | |
|---|---|
| formula | $C_{44}H_{50}N_{12}O_4S_2$ |
| $a$[Å] | 8.617(2) |
| $b$[Å] | 16.211(2) |
| $c$[Å] | 16.354(2) |
| $\alpha$[°] | 90.52(2) |
| $\beta$[°] | 105.02(3) |
| $\gamma$[°] | 97.09(2) |
| $V$[Å$^3$] | 2187.6(7) |
| $Z$ | 2 |
| formula weight | 875.1 |
| space group | $P\bar{1}$ (No. 2) |
| $T$[°C] | 25 |
| $\lambda$[Å] | 0.71073 |
| $\rho_{calcd}$[g cm$^{-3}$] | 1.328 |
| $\mu$[cm$^{-1}$] | 1.71 |
| $R$[a] | 0.089 |
| $wR_2$[b] | 0.246 |

[a] $R = \Sigma|\Delta F|/\Sigma|F_o|$. [b] $wR_2 = [\Sigma w|\Delta F^2|^2/\Sigma w|F_o^2|^2]^{1/2}$

  

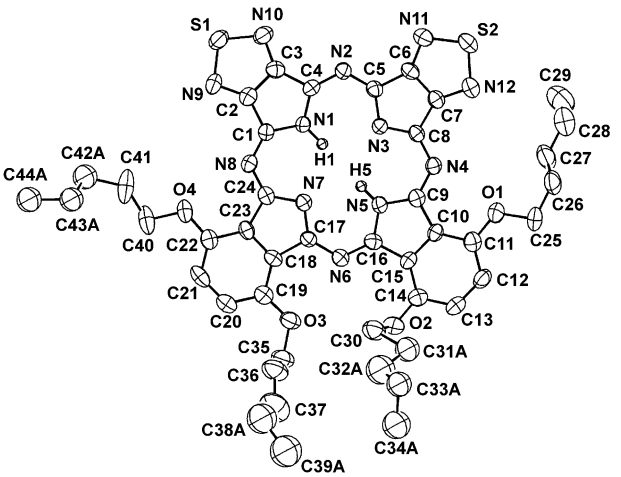


Figure 1. Structure of the *cis* species $(S_2A_2)PzH_2$ (ORTEP drawing; 30% probability ellipsoids). Disorder affecting some alkyl chains has been omitted for clarity.

solved structure of the symmetrical tetrakis(1,4-diamyloxybenzo)porphyrazine, $(A_4)PzH_2$, are also discussed.

The trend in the bond lengths and bond angles for these three macrocycles are consistent with an extended π-electron delocalization permeating the entire molecular units (with the exception of the peripheral alkyl groups). As an aid to discussions, Figure 2 details the structural features of $(S_2A_2)PzH_2$ and $(SA_3)PzH_2$. Significant differences are observed in $(S_2A_2)PzH_2$ for the separation between two pairs of opposing inner N atoms (4.043(7) Å for N1 and N5, 3.920(6) Å for N3 and N7). These separations clearly indicate that the two central hydrogen atoms are directly localized on the N1 and N5 atoms. Not unexpectedly, these findings are shared by the $(SA_3)PzH_2$ species (4.097(5) and 3.860(4) Å for distances between the opposite pyrrole and pyrrolenine N atoms, respectively; Figure 2) and its Se analogue,[8] and are also observed for the symmetrical species $(A_4)PzH_2$ (4.122(17) and 3.813(17) Å). Furthermore, in the case of $(SA_3)PzH_2$ the two internal hydrogen atoms are bound to the two opposite isoindole units that bear the electron-donating amyloxy groups. This appears to be in line with expectations, since the alternative positioning would be disfavored by the electron-withdrawing properties of the annulated 1,2,5-thiadiazole ring.

Bond lengths and angles of the inner porphyrazine skeleton in the *cis*-2:2 species $(S_2A_2)PzH_2$ and in $(A_3S)PzH_2$[8] (Figure 2) are very similar to those found in the $(A_4)PzH_2$ species.

The *cis* species $(S_2A_2)PzH_2$ offers a good opportunity for a direct comparison of the effects of the different externally annulated rings on the geometry of each individual internal

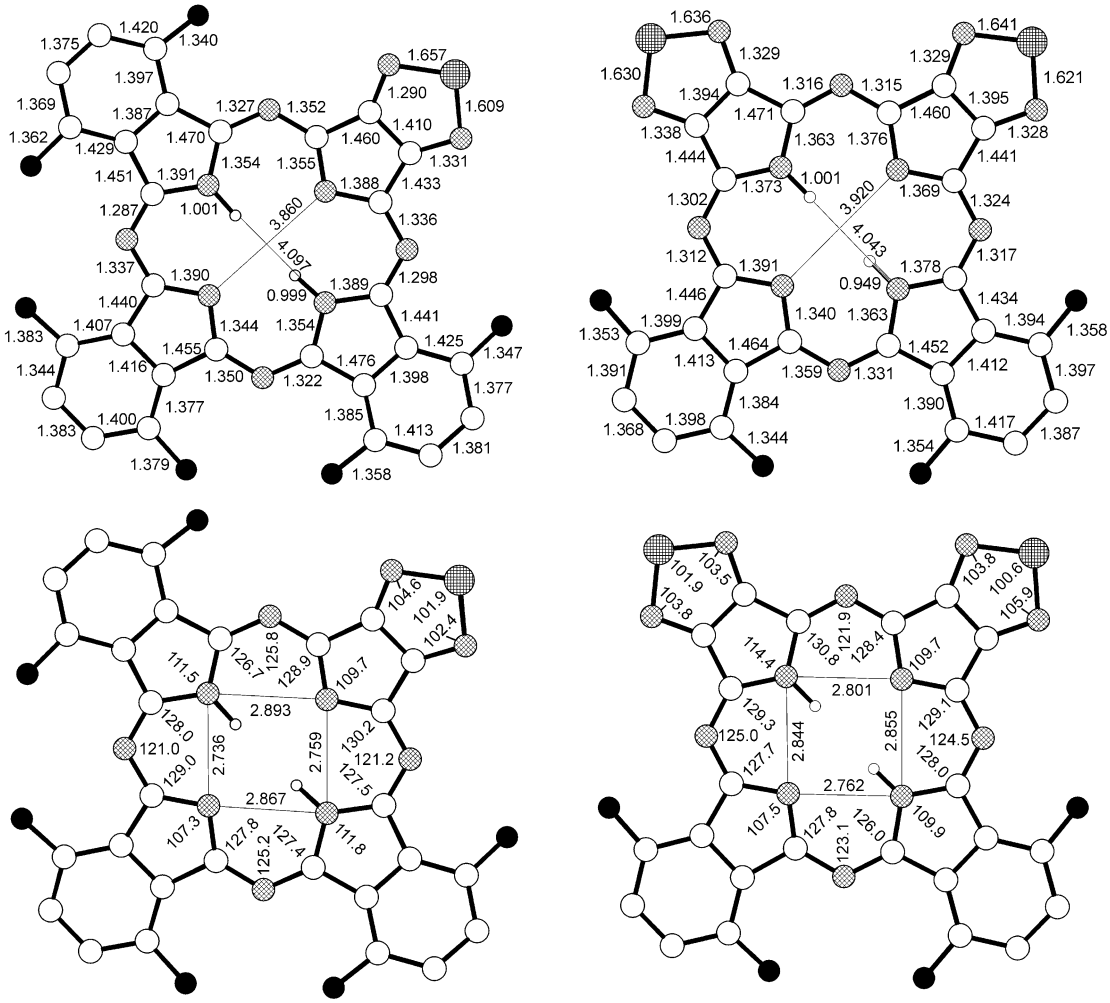


Figure 2. Top views of $(SA_3)PzH_2$ (left) and $(S_2A_2)PzH_2$ (right) with indicated values of bond lengths [Å] (top), and bond angles [°] (bottom).

pyrrole and pyrrolenine ring. First, the pyrrole ring, independent from the nature of the annulated system, has longer $N_{pyr}$–$C_\alpha$ and $C_\beta$–$C_\beta$ bonds and shorter $C_\alpha$–$C_\beta$ bonds with respect to those of the pyrrolenine ring with the same type of annulation. The pyrrole ring also has a markedly larger $C_\alpha$-$N_{pyr}$-$C_\alpha$ angle than the parent pyrrolenine ring. This effect is stronger in the case of 1,2,5-thiadiazole annulation (4°, compared with 2° in case of benzene annulation). On the other hand, in the case of heterocyclic annulation, the $N_{pyr}$–$C_\alpha$ and $C_\alpha$–$C_\beta$ bonds of both types of $C_4N$ moieties are elongated in comparison to the related values in isoindole and isoindolenine rings. These trends make it evident, that i) the π system annulated to pyrrole rings is more strongly involved in conjugation with the central 16-membered macrocyclic π system, whereas it is more isolated in pyrrolenine rings; ii) the 1,2,5-thiadiazole rings, evidently because of their strong π-deficient character, are more isolated from the central π system than the benzene rings, which are capable of π-electron donation. In view of this, it is well understood why in the case of $(SA_3)PzH_2$ the single 1,2,5-thiadiazole ring is annulated to a pyrrolenine ring and there are two isoindole moieties.

As regards the structural features of the annulated 1,2,5-thiadiazole rings in both $(S_2A_2)PzH_2$ and $(SA_3)PzH_2$, they closely resemble those of other molecules containing the 1,2,5-thiadiazole heterocycle (e.g. 2,1,3-benzothiadiazole)[32] and provide evidence that they keep the 6 π-electron aromatic system considerably isolated. For the *cis* species $(S_2A_2)PzH_2$, comparison of the bond lengths for the 1,2,5-thiadiazole ring annulated to the pyrrole and pyrrolenine rings definitely indicates shorter values for the S-containing ring in combination with the pyrrolenine ring. Again, this is indicative of the tendency of the 1,2,5-thiadiazole units to have less conjugation with the central macrocyclic π system in the case of pyrrolenine annulation.

The inner four N atoms in both $(SA_3)PzH_2$ and $(S_2A_2)PzH_2$ are practically coplanar (maximum deviation from planarity: $< 0.04$ Å). The $(A_4)PzH_2$ macrocycle is centrosymmetric; thus, the inner $N_4$ system is perfectly planar. The planarity of the $N_4$ core in all three species is consistent with the presence of bifurcated hydrogen bonds (2.10–2.30 Å), as illustrated in Figure 3 for $(S_2A_2)PzH_2$ and $(SA_3)PzH_2$. The entire macrocyclic skeleton in all species is not perfectly planar, as is also shown in Figure 3 for these two latter species.

In the symmetrical species $(A_4)PzH_2$, the steric interaction between eight amyloxy chains leads to rotation of the isoindole and especially isoindolenine units that have dihedral angles of 3.3(3) and 8.1(2)°, respectively, with the $N_4$ core. The planar distortion of the phthalocyanine macrocycle induced by amyloxy groups in this case (as well as between isoamyloxy chains in $(i\text{AmO})_8PcH_2$[33]) is much less than that reported recently[34] for the isoamyl substituted derivative $(i\text{Am})_8PcH_2$, for which dihedral angles of the two types of indole units with the $N_4$ core are 11.3° and 18.0°.

In $(SA_3)PzH_2$, the dihedral angles formed with the central $N_4$ core by the 1,2,5-thiadiazolo-pyrrolenine unit ($NC_4N_2S$), the opposite isoindolenine ring, and the two adjacent isoindole rings are 10.1(1), 8.0(1), 4.7(1), 13.5(1)°, respectively.[8] The $NC_4N_2S$ moiety and the opposite isoindolenine ring, which are nearly coplanar (dihedral angle 10.6(1)°), show a definite separation between their planes (≈0.66 Å, Figure 4). Distortion from planarity of the macrocycle in $(SA_3)PzH_2$ having six amyloxy groups is much stronger than in the case of the symmetrical $(A_4)PzH_2$ having eight amyloxy groups. This indicates that the distortion in the case of $(SA_3)PzH_2$, although certainly contributed by the steric effects of the amyloxy groups, mainly arises from the strong polarization of the π system owing to the "push–pull" interaction between the electron-deficient 1,2,5-thiadiazole ring and the strongly electron-donating amyloxy-substituted benzene rings and consequent intermolecular dipole–dipole interactions resulting in the formation of centrosymmetric molecular pairs (Figure 4). Notably, the amyloxy groups of the isoindolenine moiety in one molecule embrace the 1,2,5-thiadiazole fragment in the centrosymmetric pair. Although such conforma-

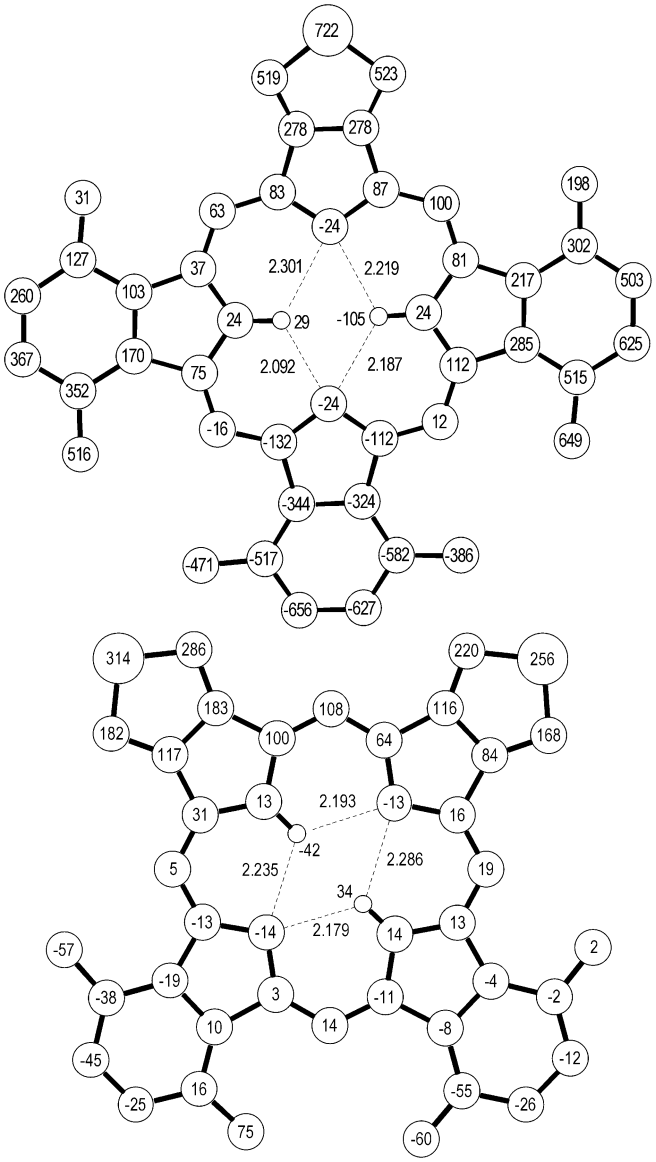


Figure 3. Deviations of atoms [$10^3$ Å] constituting the macrocyclic skeleton in $(SA_3)PzH_2$ (top) and $(S_2A_2)PzH_2$ (bottom) from the mean $N_4$ plane formed by internal nitrogen atoms and intramolecular hydrogen bonds [Å].

  

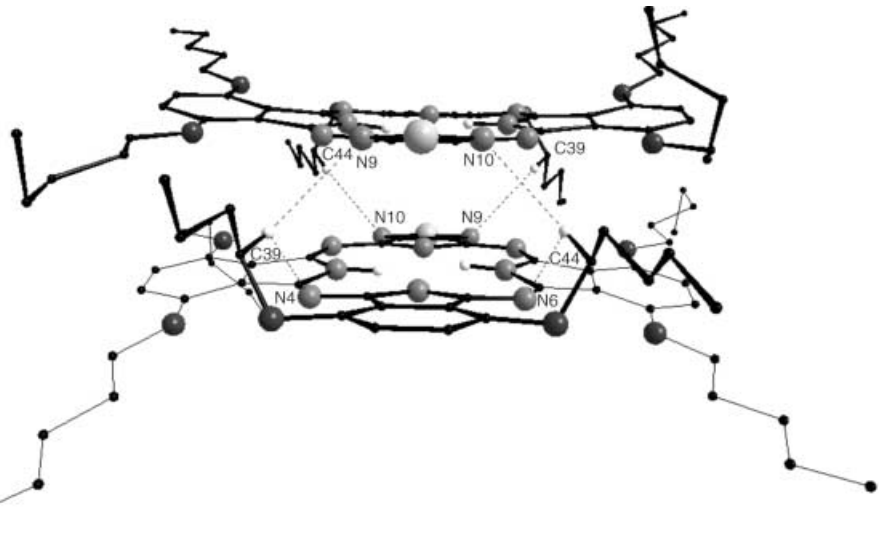


Figure 4. Inter- and intramolecular interactions in the centrosymmetric pair of $(SA_3)PzH_2$ that determine the conformation of amyloxy groups.

tion of the amyloxy groups is sterically less favorable, it allows the additional binding of the molecules in the pair by means of intermolecular interactions (weak hydrogen bonding) between the N atoms of the 1,2,5-thiadiazole ring of one molecule and H atoms of $\alpha$-$CH_2$-groups of another molecule (Figure 4). The N···HC distance is 2.67–2.80 Å, which is close to the sum of the van der Waals radii of nitrogen and hydrogen (1.55 + 1.20 = 2.75 Å). Intramolecular interactions with *meso*-N atoms ($N_{meso}$···HC: 2.54–2.80 Å) provide the additional stabilization of such a conformation of the amyloxy groups.

In the case of the *cis*-2:2 isomer $(S_2A_2)PzH_2$, the two 1,2,5-thiadiazolo-pyrrole/enine and the two isoindole/enine units containing the N1, N3, and N5, N7 atoms (Figure 1) are nearly coplanar with the mean $N_4$ plane (the dihedral angles are 2.8(1), 1.7(1), 1.3(1), and 2.5(1)°, respectively). The pairs of opposite units containing the N1, N5 and the N3, N7 atoms are also nearly coplanar. The separation between the mean planes in each pair is 0.25(3) and 0.13(3) Å, respectively, and the dihedral angle they form is 3.8(1)°. The resulting deviation of atoms constituting the inner porphyrazine macrocycle from the mean $N_4$ plane does not exceed 0.02 Å (Figure 3), except for the $C_\beta$ atoms of the pyrrole and pyrrolenine units with annulated 1,2,5-thiadiazole rings and the triatomic $C_\alpha$-$N_{meso}$-$C_\alpha$ bridge between them, whose displacement is caused by ruffling of the thiadiazole rings that are located above the mean plane. Despite the ruffling, the deviation of the S atoms (0.314 and 0.256 Å in the heterocycles annulated to pyrrole and pyrrolenine rings, respectively) remains less than for $(SA_3)PzH_2$ (0.722 Å). As observed for $(SA_3)PzH_2$, the amyloxy groups in $(S_2A_2)PzH_2$ are also involved in weak intermolecular hydrogen bonding (see frontispiece).

As shown in Figure 5, the crystal packing of $(S_2A_2)PzH_2$ consists of molecular layers running parallel to the (110) plane. In this arrangement, pairs of centrosymmetric molecules are oriented in such a way that the nitrogen atom N3 (Figure 1) of one molecule overlaps the benzene ring of the isoindolenine unit containing N7 of the adjacent molecule. The molecules in a pair, and the adjacent interpair molecules as well, approach each other at an interplanar distance of 3.273(10) Å. Such an intermolecular distance is appreciably shorter than that found in a number of simple phthalocyanine systems (3.30–3.40 Å) and might be indicative of some π–π intermolecular interaction, a prerequisite for some charge transfer occurring along the columnarly stacked system, with possible manifestation of some electrical conductivity properties. Unfortunately, the very small amounts of pure *cis* species available did not allow any solid-state electrical conductivity measurements to be carried out. It is interesting that pairs of molecules similar to those found for the *cis* species are also present in the species $(SA_3)PzH_2$ with an identical intermolecular distance within the pair (3.273(10) Å).[8] In the latter, however, the pairs are distributed differently within the cell, in such a way (Figure 6) that there are no significant contacts between themselves. Thus there is only a low probability of an efficient long-distance electronic charge transmission.

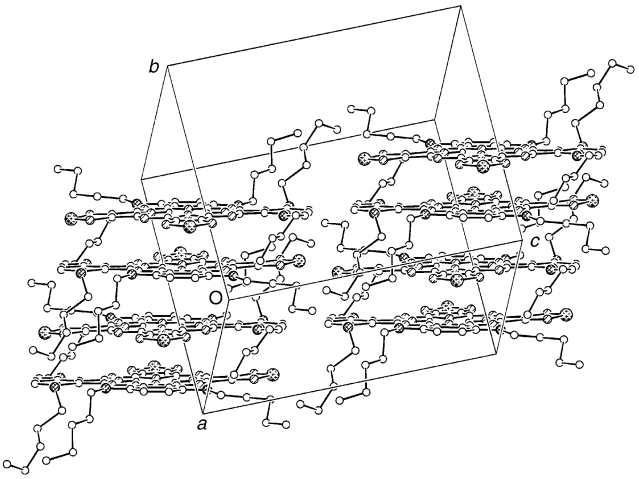


Figure 5. The packing of the species $(S_2A_2)PzH_2$ (SCHAKAL view). Disorder affecting some alkyl chains has been omitted for clarity.

The packing of the symmetrical species $(A_4)PzH_2$ consists of infinite chains of adjacent molecules parallel to the (110) plane (Figure 7). The distance between adjacent planes is 3.535(19) Å and the molecules are only very rarely superimposed.

**IR spectra**: The IR spectra of the present series of unsymmetrical porphyrazines are given in Figure 8 together with the spectra of the symmetrical species. In the spectrum of $(A_4)PzH_2$ (Figure 8F) the vibrations of the eight amyloxy groups ($\nu(CH)_{Am} = 2850–2960\ cm^{-1}$, $\delta(CH)_{Am} = 1465$ and

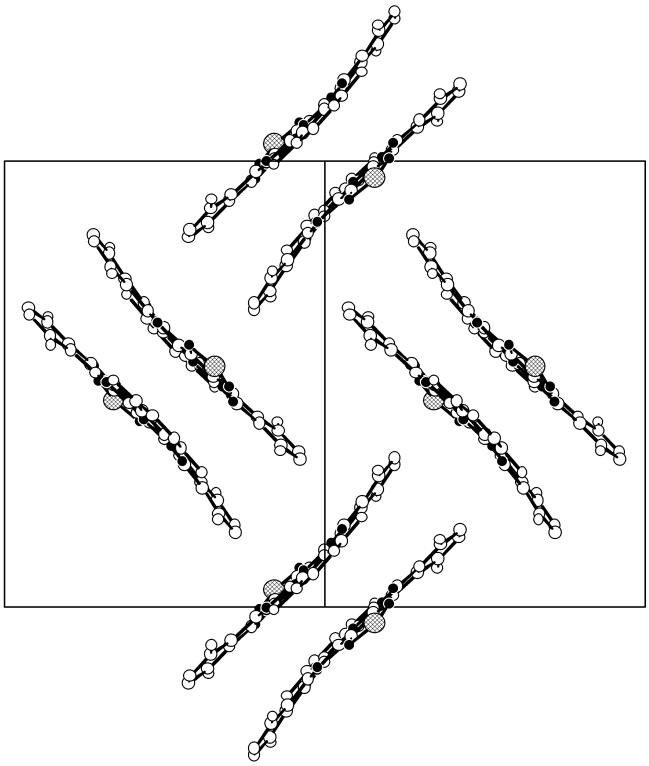

Figure 6. View of the unit cell of $(SA_3)PzH_2$ along the (101) axes. Alkyl chains are omitted for clarity.

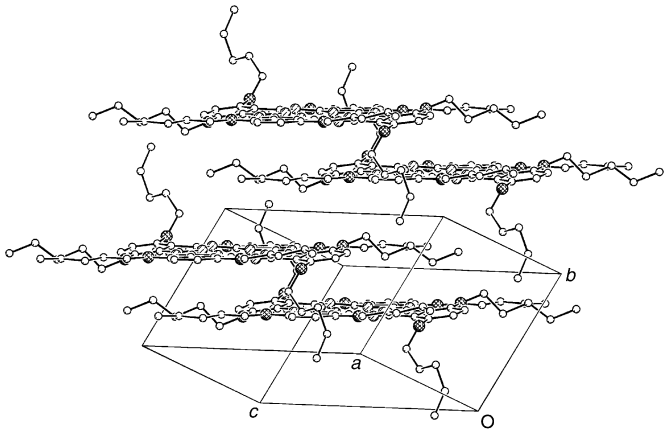


Figure 7. The packing of $(A_4)PzH_2$ (SCHAKAL view). Disorder affecting some alkyl chains has been omitted for clarity.

1376 cm$^{-1}$, $\nu$(C–O)$_{arom}$ = 1260–1270 cm$^{-1}$ and $\nu$(O–Am) = 1020–1060 cm$^{-1}$) and of the four benzene rings ($\nu$(C:C) = 1600 and 1500 cm$^{-1}$, $\gamma$(CH) = 876 cm$^{-1}$)[35] produce the most intense bands which strongly overlay the skeleton vibrations of the internal porphyrazine core. Annulation of 1,2,5-thiadiazole rings instead of diamyloxy-substituted benzene rings results in the decrease of the intensity of the above-mentioned bands and in the appearance of the characteristic bands assigned to vibrations of the 1,2,5-thiadiazole rings ($\nu$(S–N) at 750–760 and 810–820 cm$^{-1}$, $\nu$(C=N), and $\nu$(C:C) at 1215 and 1265 cm$^{-1}$, ring deformations at 510–520 cm$^{-1}$).[6] The vibrations of the porphyrazine skeleton also become distinctly visible ($\nu$(C:N$_{meso}$) at 1530 cm$^{-1}$, pyrrole ring vibrations at 1130 and 1010–1060 cm$^{-1}$). In the case of the *cis*-arranged species $(S_2A_2)PzH_2$, in which two types of the 1,2,5-thiadiazole ring are present (annulated to pyrrole and to pyrrolenine rings) their torsion vibrations give a double band (498 and 512 cm$^{-1}$).

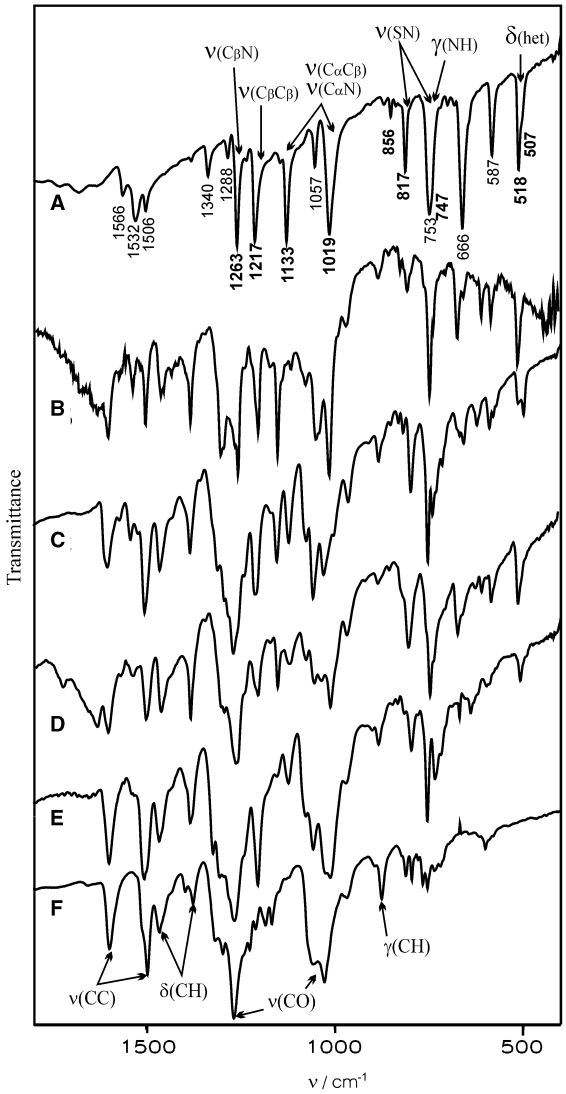


Figure 8. IR spectra of $(S_4)PzH_2$ (A), $(S_3A)PzH_2$ (B), $(S_2A_2)PzH_2$ (C), $(SASA)PzH_2$ (D), $(SA_3)PzH_2$ (E), and $(A_4)PzH_2$ (F). For $(S_4)PzH_2$, bold-type wavenumbers indicate vibrations of 1,2,5-thiadiazole rings and, strongly coupled with them, pyrrole ring vibrations. The assignments for vibrations of the amyloxy groups are shown for $(A_4)PzH_2$.

**$^1$H NMR spectra**: The amyloxy chains present in the porphyrazines $(A_4)PzH_2$, $(SA_3)PzH_2$, $(S_2A_2)PzH_2$, and $(SASA)PzH_2$ endow them with sufficient solubility to allow the measurement of their $^1$H NMR spectra in neutral solvents ($CDCl_3$). In the case of the 3:1 porphyrazine macrocycle, only the spectrum of the Mg derivative $[(S_3A)PzMg]$ in $[D_5]$pyridine could be obtained. A comparison of the observed chemical shifts is presented in Table 2. The aromatic protons of the benzene rings give resonances in the region $\delta$ = 7.1–7.7 ppm and the number of signals and their position are characteristic for each species. Only one signal in the aromatic region is observed for the symmetrical species $(A_4)PzH_2$, and for *trans*-2:2 and 3:1 low-symmetry porphyrazines. In the case

  

Table 2. Chemical shifts ($\delta$) in the $^1$H NMR spectra of porphyrazines with annulated 1,2,5-thiadiazole rings in $CDCl_3$.

| | Compound | CH | $\alpha$-$CH_2$ | $\beta$-$CH_2$ | $\gamma$-$CH_2$ | $\delta$-$CH_2$ | $CH_3$ | NH |
|---|---|---|---|---|---|---|---|---|
| **7a** | $(A_4)PzH_2$ | 7.60 (s, 8H) | 4.85 (t, 16H) | 2.27 (qt, 16H) | 1.72–1.40 (m, 32H) | | 0.99 (t, 24H) | 0.26 (2H) |
| **3a** | $(SA_3)PzH_2$ | 7.66 (s, 2H) | 4.82 (t, 4H) | 2.42 (m, 4H) | 1.75–1.40 (m, 24H) | | 1.11 (t, 6H) | −0.25 (s, 2H) |
| | | 7.65 (s, 2H) | 4.78 (t, 4H) | 2.22 (m, 8H) | | | 0.97 (t, 6H) | |
| | | 7.51 (s, 2H) | 4.67 (t, 4H) | | | | 0.86 (t, 6H) | |
| **4a** | $(S_2A_2)PzH_2$ | 7.17 (d, 2H) | 4.60 (t, 4H) | 2.28 (m, 4H) | 1.88 (m, 4H) | 1.40–1.60 (m, | 1.12 (t, 6H) | −1.83 (s, 2H) |
| | | 7.21 (d, 2H) | 4.42 (t, 4H) | 2.14 (m, 4H) | 1.69 (m, 4H) | 8H) | 1.06 (t, 6H) | |
| **5a** | $(SASA)PzH_2$ | 7.45 (s, 4H) | 4.72 (t, 4H) | 2.38 (m, 4H) | 2.01 (m, 4H) | 1.45–1.65 (m, | 1.13 (t, 6H) | −0.87 (s, 2H) |
| | | 4.57 (t, 4H) | 2.21 (m, 4H) | 1.71 (m, 4H) | 8H) | 1.02 (t, 6H) | | |
| **5b** | [(SASA)PzMg] | 7.14 (s, 4H) | 4.09 (t, 8H) | 1.83 (qt, 8H) | 1.39 (m, 16H) | 0.90 (t, 12H) | | |
| **6b** | $[(S_3A)PzMg]$[a] | 7.66 (s, 2H) | 4.66 (t, 4H) | 2.39 (m, 4H) | 2.10 (m, 4H) | 1.69 (m, 4H) | 0.75 (t, 6H) | |

[a] In $[D_5]$pyridine.

of $(SA_3)PzH_2$ and $(S_2A_2)PzH_2$, which have lower symmetry, the nonequivalent benzene protons show, correspondingly, three singlets and a double doublet. Introduction of the π-electron deficient 1,2,5-thiadiazole rings leads to polarization of the macrocyclic π system and reduces the local π-ring currents in the benzene rings. As a result, the signal of the benzene protons in the low-symmetry porphyrazines is shifted upfield. This effect is especially pronounced for the *cis*-2:2 species. Owing to the deshielding effect of the macrocyclic π-ring current, the aliphatic protons of the amyloxy groups give well-separated signals: $\alpha$-$CH_2$ triplets at $\delta = 4.0-4.9$ ppm, $\beta$-$CH_2$: quintets at $\delta = 1.8-2.4$ ppm, $\gamma$-$CH_2$ multiplets at $\delta = 1.7-2.1$ ppm, $\delta$-$CH_2$: multiplets at $\delta = 1.4-1.6$ ppm and terminal $CH_3$ group triplets at $\delta = 0.75-1.15$ ppm. Because the amyloxy groups are not equivalent in $(SA_3)PzH_2$ and $(S_2A_2)PzH_2$, the former species exhibits three groups of multiplets for $\alpha$-$CH_2$, $\beta$-$CH_2$ and $CH_3$ protons, and for the latter, two multiplets appear for $\alpha$-, $\beta$-, $\gamma$-$CH_2$, and $CH_3$ protons. Unexpectedly, also the *trans* species $(SASA)PzH_2$, which carries four chemically equivalent amyloxy groups, gives two multiplets for each $\alpha$-, $\beta$-, and $\gamma$-$CH_2$, and $CH_3$ protons. Such magnetic anisotropy can evidently arise from the fixed conformation of the amyloxy groups on account of their weak intramolecular hydrogen-bonding interaction with the N atoms located in the *meso* positions and in the adjacent heterocyclic rings: this is similar to that observed in the crystalline state for 1:3 and *cis*-2:2 species (see above). It is also possible that, at the concentration level used for $^1$H NMR spectroscopy ($\approx 10^{-3}$ M), dimerization might occur. Interestingly, for the Mg derivative [(SASA)PzMg] all signals are shifted upfield and no splitting is observed.

The internal NH protons of the free bases, being shielded by the macrocyclic π-ring current, give broad singlets in the high field region (at $\delta = -2$ to 0.3 ppm). It is known that the chemical shift for the NH protons in porphyrazines is strongly influenced not only by the macrocyclic π-ring current, but also by aggregation effects[36] and by acidity of the N–H bonds and the resulting intramolecular hydrogen bonding.[37] The observed deviation of the N–H bonds from the mean plane of the macrocycle (Figure 3) can also have a considerable influence on the chemical shift. For $(S_2A_2)PzH_2$, the NH protons resonate at a higher field than in the case of the more distorted $(SA_3)PzH_2$ and of the symmetrical species $(A_4)PzH_2$. The singlet observed for the NH protons in $(S_2A_2)PzH_2$ is probably the result of a rapid exchange process. In this case, lowering of the temperature results in the downfield shift and broadening of the NH resonance (Figure 9), which disappears at −48 °C. At −58 °C, two very broad signals at $\delta - 0.7$ and $-1.4$ ppm appear, but their complete

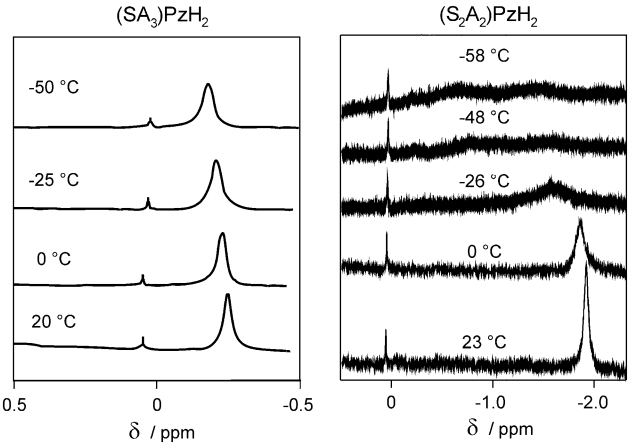


Figure 9. Temperature dependence of the NH-proton resonance in the $^1$H NMR spectra of $(SA_3)PzH_2$ (left) and $(S_2A_2)PzH_2$ (right). Solvent: $CDCl_3$.

reappearance requires a lower temperature which is not possible in $CDCl_3$. Very strong broadening and a low-field shift is also observed for the signal of aromatic CH protons. In the case of $(SA_3)PzH_2$, in agreement with the X-ray results, the internal H atoms are fixed on the more electron-rich isoindole moieties, and even at −50 °C no splitting or broadening of the NH resonance is observed; it only shifts from $\delta = -0.25$ ppm at 20 °C to $\delta = -0.18$ ppm at −50 °C and the three aromatic CH singlets retain their sharpness. Also for the *trans*-2:2 porphyrazine, it is evident that there is only one isomer with two isoindole rings.

**UV/Vis spectra and acid–base properties**: The UV/Vis spectra of the unsymmetrical porphyrazines $(S_3A)PzH_2$, $(S_2A_2)PzH_2$, and $(SA_3)PzH_2$ are shown in Figure 10 (solid lines), together with those of the symmetrical species $(S_4)PzH_2$ and $(A_4)PzH_2$. In a way similar to that of the phthalocyanine macrocycles, they are all characterized by the presence of intense absorptions assigned to $\pi \rightarrow \pi^*$ transitions in the visible or near-IR regions (*Q* bands) and in the UV region (*B* bands). Annulation of the amyloxy-substituted benzene rings

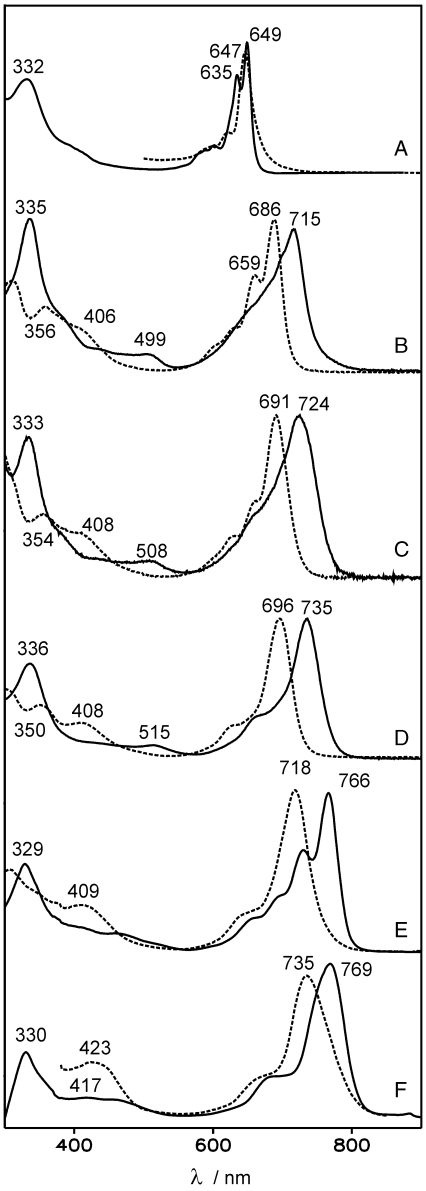


Figure 10. UV/Vis spectra of $(S_4)PzH_2$ (A), $(S_3A)PzH_2$ (B), $(SASA)PzH_2$ (C), $(S_2A_2)PzH_2$ (D), $(SA_3)PzH_2$ (E) and $(A_4)PzH_2$ (F) in $CH_2Cl_2$ (——) and of their deprotonated forms obtained in the presence of tba(OH) (- - - -).

in place of the 1,2,5-thiadiazole rings leads to the increasing bathochromic shift of the *Q*-band maxima ($649 \rightarrow 715 \rightarrow 724 \rightarrow 735 \rightarrow 766 \rightarrow 769$ nm, for $(S_4)PzH_2$, $(S_3A)PzH_2$, $(SASA)PzH_2$, $(S_2A_2)PzH_2$, $(SA_3)PzH_2$, $(A_4)PzH_2$, respectively), but produces minor changes in the position of the *B*-band maxima located at ≈330 nm. The amyloxy-substituted benzene rings act as strong electron donors to the porphyrazine macrocycle, and their replacement by the π-electron-deficient 1,2,5-thiadiazole rings leads to destabilization of the HOMO, whereas the energy of HOMO-1 and LUMO is influenced only slightly by substituents in the *β*-pyrrole positions.

With regard to the complete series of free ligands depicted in Scheme 2, the symmetry of the macrocyclic π-chromophore is $D_{2h}$, as is the case for $(S_4)PzH_2$, $(A_4)PzH_2$ and $(SASA)PzH_2$, or lower. As a result, the *Q* band has, respectively, either the expected characteristic splitting, as occurs for $(S_4)PzH_2$ and $(SA_3)PzH_2$ (spectra A and E, Figure 10), or asymmetry, as is evident for $(S_3A)PzH_2$, $(SASA)PzH_2$ and $(A_4)PzH_2$ (spectra B, C and F, Figure 10). Interestingly, for the *Q* band of the *cis*-2:2 isomer $(S_2A_2)PzH_2$ (Figure 10D,) no splitting is observed, unlike the *trans* isomer $(SASA)PzH_2$ which is characterized by a broadened hypsochromically shifted *Q*-band envelope.

The unsymmetrical macrocycles $(SA_3)PzH_2$, the 2:2 isomers, and $(S_3A)PzH_2$, like $(S_4)PzH_2$, can be considered to be multicenter conjugated ampholites because they contain two acidic internal N–H groups as well as several basic centers, namely the four *meso*-N atoms and the N atoms of the 1,2,5-thiadiazole rings. This results in a peculiar behavior of these species in the presence of acids and bases and in the solvents with different proton-donor and proton-acceptor abilities, as is briefly discussed here below.

First, addition of strong bases such as tetra(*n*-butyl)ammonium hydroxide, [tba]OH, to solutions of the species $(SA_3)PzH_2$, either 2:2 isomers, and $(S_3A)PzH_2$ in neutral solvents ($CH_2Cl_2$, $CHCl_3$) leads to deprotonation and formation of the corresponding dianions with associated changes in the UV/Vis spectra (Figure 10, dashed lines). The position of the *Q*-band maxima is shifted hypsochromically by 30–50 nm (600–900 $cm^{-1}$) owing to destabilization of the LUMO in the dianions so that the *Q* absorptions become definitely more narrow than for the free bases because of the rise in the symmetry of the π-chromophore. The position of the *B* band is generally shifted bathochromically because of the large destabilization of the HOMO-1.

In pyridine solutions, the dissociation of the central NH groups and the related spectral response is clearly a function of the specific nature of the macrocycle considered. As already reported by us,[3] the free ligand $(S_4)PzH_2$ forms the pyridinium saltlike species $[(S_4)Pz]^{-2}(pyH^+)_2$ as a consequence of the presence of four annulated 1,2,5-thiadiazole rings that favor dissociation. Identical behavior is shown by $(S_3A)PzH_2$ immediately after dissolution in the N base. On the contrary, $(A_4)PzH_2$ and $(SA_3)PzH_2$ show no tendency to dissociate, evidently as a result of the effect on NH dissociation caused by the prevalent presence of the electron-donating amyloxy groups. Both 2:2 isomers exhibit intermediate behavior, since they show some interaction with pyridine only after prolonged heating.

As shown for other porphyrazines,[38–40] protonation of the donor *meso*-N atoms can occur in acidic media, leading to a bathochromic shift of the *Q*-band maxima by 500–1500 $cm^{-1}$ for each N atom involved. Unlike protonation of *meso*-nitrogens, their acid solvation as well as acid–base interaction with N atoms of annulated heterocyclic rings have only a minor solvatochromic effect (±300 $cm^{-1}$). It was also shown that, unlike common porphyrins, protonation of internal pyrrolenine nitrogen atoms is not usually observed for porphyrazines.[38, 40]

UV/Vis spectra in acidic media of a series of species with differing numbers of peripheral substituents are displayed in Figure 11. For the symmetrical octaamylate $(A_4)PzH_2$, as occurs for the unsubstituted phthalocyanine, $PcH_2$,[38] stepwise protonation of all four *meso*-N atoms is observed on increasing the acidity of the media upon going from neutral $CH_2Cl_2$, to formic and trifluoroacetic acid, and finally to

  

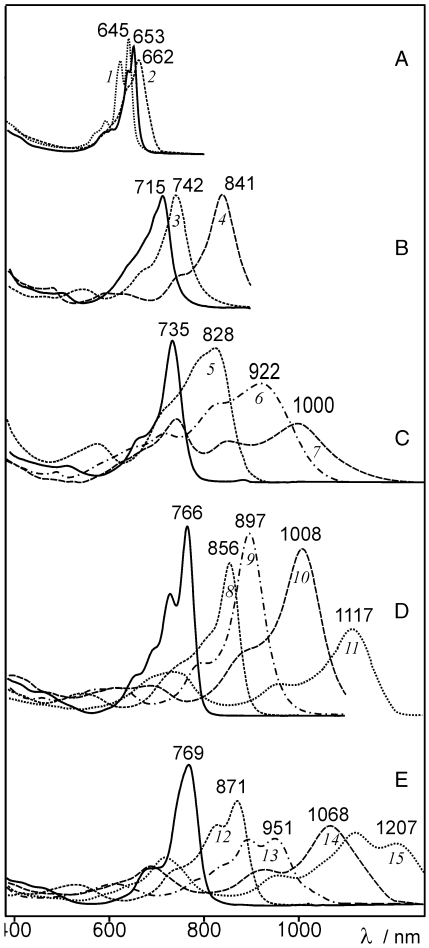


Figure 11. UV/Vis spectra of $(S_4)PzH_2$ (A) in chlorobenzene, $(S_3A)PzH_2$ (B), $(S_2A_2)PzH_2$ (C), $(SA_3)PzH_2$ (D) and $(A_4)PzH_2$ (E) in $CH_2Cl_2$ (——) and of their acid associated and protonated forms obtained in acid media—in $CH_2Cl_2$ containing HCOOH 0.5 % (12), 5 % (8,13), 100 % (9), in $CF_3COOH$ (1,3,5), in $CF_3COOH$ containing 1 % $H_2SO_4$ (6,14), in $CH_3COOH$ containing 35 % $H_2SO_4$ (10) and in 96 % aqueous $H_2SO_4$ (2, 4, 7, 11, 15).

concentrated $H_2SO_4$. A bathochromic shift of the *Q* band by 700 – 1500 $cm^{-1}$ can be observed in correspondence with each protonation step, with the *Q*-band maximum for the tetraprotonated form (in $H_2SO_4$) being shifted by more than 4700 $cm^{-1}$ (1207 nm). In $(S_4)PzH_2$, the basicity of the *meso*-N atoms is markedly quenched by the effect of the 1,2,5-thiadiazole rings present. Accordingly, only "acid solvation" was evidenced for $(S_4)PzH_2$ in $CF_3COOH$,[3] with a subtle hypsochromic shift of the *Q* band ($\approx$200 $cm^{-1}$), and protonation of only one *meso*-N atom takes place ($pK_{a1} = -4.06$) in the strongly acidic 96 % $H_2SO_4$ (bathochromic shift of the *Q* band $\approx$400 $cm^{-1}$), the second protonation step ($pK_{a2} < -13$) can be observed only in more strongly acidic media (> 100 % $H_2SO_4$, oleum, $HSO_3Cl$).[41] Inspection of the UV/Vis spectra of the unsymmetrical porphyrazines $(S_3A)PzH_2$, $(S_2A_2)PzH_2$ and $(SA_3)PzH_2$ with increasing acidity of the media ($CH_2Cl_2 \rightarrow HCOOH \rightarrow CF_3COOH \rightarrow H_2SO_4$, see Figure 11) shows the formation of two (bathochromic shift 2100 $cm^{-1}$ in $H_2SO_4$), three (3600 $cm^{-1}$), and four acid forms (4100 $cm^{-1}$), respectively.

It is known,[38] that delocalization of the positive charge of the acid forms along the π system of the porphyrazine macrocycle results in a bathochromic shift of the *Q* band by 400 – 700 $cm^{-1}$ for each progressive protonation step, whereas involvement of peripheral substituents in delocalization, especially benzene rings having strong electron-buffering properties, increases the value of the shift up to $\approx$1300 $cm^{-1}$. The observed values of the bathochromic shifts of the *Q* band indicate that for the monoprotonated forms the positive charge is delocalized within the porphyrazine π system for $(S_4)PzH_2$ and $(S_3A)PzH_2$, whereas for both 2:2 species, that is, $(S_2A_2)PzH_2$ and $(SASA)PzH_2$, as well as for $(SA_3)PzH_2$ and $(A_4)PzH_2$, the π system of the benzene rings is strongly involved in delocalization.

As indicated by UV/Vis spectral features, annulation of the electron-withdrawing 1,2,5-thiadiazole rings instead of the benzene rings results in a lowering of the basicity of the porphyrazine macrocycle. Whereas the monoprotonated form of $(A_4)PzH_2$, $(SA_3)PzH_2$, and of both 2:2 isomers can be obtained in $CH_2Cl_2$ containing increasing amounts of HCOOH (0.5, 5, 50 %, respectively), protonation of the first *meso*-nitrogen atom in $(S_3A)PzH_2$ can be observed only in 100 % $CF_3COOH$, and in the case of $(S_4)PzH_2$ only in concentrated $H_2SO_4$.[3, 41]

**Nonlinear optical properties**: Nonlinear transmission is a nonlinear optical property of materials which allows one to control the energy of laser pulses. Among different materials with nonlinear optical properties, nonlinear absorbers are particularly useful in applications, such as optical limiting, which can be used for eye protection, or more generally, optical detector protection and also in photonic devices.[42] Several mechanisms at the molecular level are the basis for an optical limiter and of particular importance is a sequential two-photon absorption like a reverse saturable absorption (RSA) mechanism, in which excited states absorb more than the ground state, since a low threshold for the non-linearity is usually found.

Molecular structures such as phthalocyanines[43, 44] and porphyrins[45, 46] have been identified as very active RSA molecules useful for limiting laser pulses on the nanosecond time scale and in the visible frequency range, particularly at 532 nm (the doubled frequency of a Nd:YAG laser), since the lowest triplet state is efficiently populated within nanoseconds and it shows an absorption maximum at $\approx$500 – 550 nm where the ground state has a low absorption. Owing to the phthalocyanine-type structure of the present symmetrical and unsymmetrical new species, the optical limiting behavior of the series $(A_4)PzH_2$, $(SA_3)PzH_2$, $(S_2A_2)PzH_2$, and $(S_4)PzH_2$ was investigated.

The first three molecules are soluble in toluene and the trend of the optical limiting response of their solutions in this medium is shown in Figure 12. Measurements were carried out with 9-ns pulses at 532 nm from a doubled Nd:YAG laser. Since the systems behave as RSA and the molecular population accumulates in the triplet states with long lifetimes with respect to the laser pulses, the fluence rather than the intensity of the laser pulses was the appropriate quantity to be considered. It is clear from Figure 12 that solutions with almost equal transmittance at 532 nm show very different optical limiting behavior. The symmetrical species $(A_4)PzH_2$

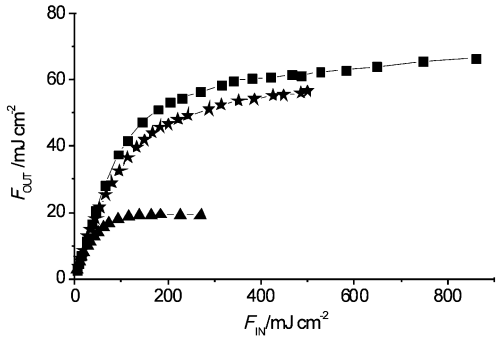


Figure 12. Optical limiting curves for $(A_4)PzH_2$ (▲), $(SA_3)PzH_2$ (*) and $(S_2A_2)PzH_2$ (■) in toluene solution with 56, 60, and 54% linear transmittance, respectively, at 532 nm in a 0.2-cm quartz cell; 9-ns laser pulses at 532 nm were used for the measurements.

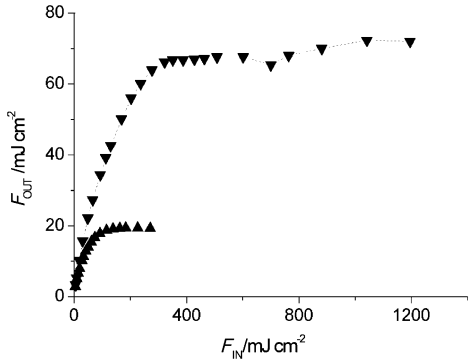


Figure 14. Optical limiting curves for $(A_4)PzH_2$ in toluene (▲) and toluene/DMSO (1:1) (▼) solutions with 56% linear transmittance at 532 nm in a 0.2 cm quartz cell; 9-ns laser pulses at 532 nm were used for the measurements.

shows the best performance and the limit of the curve coincides with the initial decomposition of the macrocycle. This happens at lower fluences with respect to the other porphyrazines, since the large nonlinear absorption results in a large quantity of local heat transfer to the solvent which has a finite dispersion capacity. The measurements for the low-symmetry species $(SA_3)PzH_2$ and $(S_2A_2)PzH_2$ show that an increase of the S-containing peripheral rings lowers the optical limiting performance.

The symmetrical porphyrazine $(S_4)PzH_2$ was found to be practically insoluble in toluene, and a little higher solubility was found for a solution in 1:1 toluene/DMSO. Figure 13 shows the optical limiting behavior of such solutions for

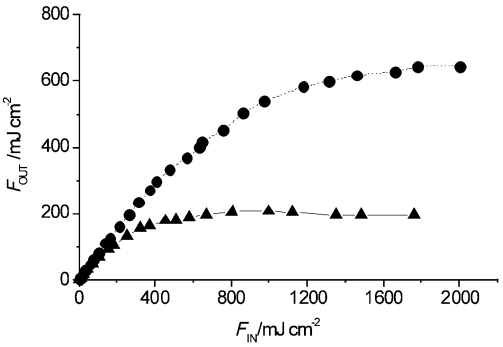


Figure 13. Optical limiting curves for $(A_4)PzH_2$ (▲) and for $(S_4)PzH_2$ (●) in toluene/DMSO (1:1) solution with 79 and 81% linear transmittance, respectively, at 532 nm in a 0.2-cm quartz cell; 9-ns laser pulses at 532 nm were used for the measurements.

$(S_4)PzH_2$ and $(A_4)PzH_2$. It is observed that the performance of the porphyrazine $(S_4)PzH_2$ is lower than that of the phthalocyanine $(A_4)PzH_2$, in agreement with the above results. Figure 14 compares the optical limiting behavior of $(A_4)PzH_2$ in pure toluene and in the 1:1 toluene/DMSO mixture. It seems that the presence of DMSO lowers the optical limiting performance; this is presumably the result of a specific solute–solvent interaction.

In summary, the above results indicate that progressive introduction of the thiadiazole rings in the macrocycle disfavors the optical limiting performance. The reason for such behavior should be related to the RSA mechanism involving the triplet-to-triplet absorption, which is characteristic of this type of structures. The structural modification along the series clearly implies a parallel change in the electronic properties of the molecules, as is clear from the UV/Vis electronic spectra (Figure 10), and one should consider that the triplet-to-triplet absorption spectrum can also be changed in frequency and/or that its absorption cross-section may undergo some modification. On the other hand, the intersystem crossing efficiency might also be affected. Preliminary pump & probe measurements with the same laser pulses used for the optical limiting measurements indicate that the excited-state spectrum of $(A_4)PzH_2$ shows a maximum absorption cross-section at $\approx$550 nm, which is consistent with the triplet-to-triplet absorption usually found for phthalocyanines.[44] The excited-state spectrum of $(S_2A_2)PzH_2$, on the other hand, shows a similar band structure, with a maximum slightly shifted to higher frequencies, but with lower transient absorption. This observation justifies the measured optical limiting behavior of the two species $(A_4)PzH_2$ and $(S_2A_2)PzH_2$ and indicates that the same RSA mechanism is present for the two molecules, although one cannot decide, at present, if the lower efficiency observed for $(S_2A_2)PzH_2$ is caused by a variation of the intersystem crossing efficiency and/or a variation of the absorption cross-section of the triplet state.

## Conclusion

Synthetic work has led to the isolation and characterization of new symmetrical and unsymmetrical Mg and related free-base porphyrazine macrocycles containing peripherally annulated 1,2,5-thiadiazole and 1,4-diamyloxybenzene moieties. The structural information obtained by elucidation of the structures of three out of the six possible components of the series of the free-base macrocycles by single-crystal X-ray diffraction has demonstrated the role played by the annulated electron-deficient (thiadiazole) and electron-donor (diamyloxybenzene) fragments in determining the solid-state intra- and intermolecular arrangements. The different electronic situation present in the various species along the series also has a remarkable effect on their properties in solution, as is

  

especially evidenced by the characteristic UV/Vis spectral features (especially in the *Q*-band region) and by their acid–base behavior in media of different acidity. The nonlinear transmission properties (optical limiting behavior), which depend on the excited-states dynamics, are also strongly influenced by the new electronic situation. Noticeably, low-symmetry features of the macrocycles do not seem to improve the optical limiting response; this is probably related to the intrinsic nature of the electron-withdrawing thiadiazole rings. Future measurements on the second-order nonlinear properties will presumably provide a better illustration of the effect of the noncentrosymmetric structure of some molecules and, in particular, of the occurring intramolecular "push–pull" effect.

## Experimental Section

**Materials**: All chemicals and solvents were reagent grade.

**Synthetic procedures**: 1,2,5-Thiadiazole-3,4-dicarbonitrile (**1**) and $(S_4)PzH_2$ (**8a**) were prepared as described elsewhere.[3] Slightly different methods, with respect to those outlined previously,[47] were used for the synthesis of 3,6-diamyloxyphthalodinitrile (**2**) and the octaamyloxyphthalocyanine, $(A_4)PzH_2$ (**7a**).

**3,6-Diamyloxyphthalodinitrile (2)**: 2,3-Dicyanohydroquinone (3.2 g, 0.02 mol), anhydrous potassium carbonate (13.8 g), and amyl bromide (7.5 mL, 0.06 mol) were suspended in DMF (40 mL), and the mixture was heated at 110 °C for 16 h. After the mixture was cooled and filtered, the white crystalline solid was washed with water until the washings were colorless, and then dried to constant weight in a vacuum. Yield: 5.51 g (92 %); elemental analysis calcd (%) for $C_{18}H_{24}N_2O_2$: C 71.97, H 8.05, N 9.32; found: C 71.51, H 8.43, N 9.37.

**1,4,6,9,11,14,16,19-Octaamyloxyphthalocyanine, $(A_4)PzH_2$ (7a)**: 3,6-Diamyloxyphthalodinitrile (**2**) (2 g, 6.66. mmol) was suspended under nitrogen in amyl alcohol (50 mL) and heated at 120 °C until complete dissolution of the solid. Lithium (0.152 g, 21.9 mmol) was added to the hot solution and the mixture was refluxed for 2 h under a $N_2$ atmosphere. After the mixture had been cooled, glacial acetic acid (5 mL) and acetone (100 mL) were added to the green solution, which changed its color to purple. The precipitate formed was separated by filtration under vacuum, washed with acetone, and dried (yield: ≈600 mg). Portions of this solid were purified by chromatography as needed (silica gel; $CHCl_3$ and ether as eluents), allowing the separation of a green fraction from which pure solid $(A_4)PzH_2$ was obtained after evaporation of the solvent mixture. IR (KBr): $\tilde{\nu} = 3296$ w (NH); 3066 vw $(CH)_{arom}$; 2954 m, 2925 m, 2869 m, 2857 m $(CH)_{Am}$); 1598 s, 1497 s $(CC)_{arom}$; 1465 m, 1376 m ($\delta(CH)_{Am}$); 1268 vs $(C-O)_{arom}$; 1184 w, 1167 w; 1058 s, 1027 s (O–Am); 968 w, 876 m, 812 w, 795 w, 767 w, 754 w, 601 w $cm^{-1}$; UV/Vis (toluene): $\lambda_{max}$ ($\log\varepsilon$) = 329(4.69), 402(4.31), 667(4.46), 695(4.51), 739(5.01), 762 nm (5.09); $^1H$ NMR ($CDCl_3$): $\delta = 0.26$ (s, 2H, NH), 0.99 (t, $J = 7.0$ Hz, 24H, $CH_3$), 1.40–1.72 (m, 32H, $\delta$- and $\gamma$-$CH_2$), 2.27 (qt, $J = 7.3$ Hz, 16H, $\beta$-$CH_2$), 4.85 (t, $J = 7.7$ Hz, 16H, $\alpha$-$CH_2$), 7.60 ppm (s, 8H, CH); elemental analysis calcd (%) for $C_{72}H_{98}N_8O_8$ (1203.6): C 71.85, H 8.21, N 9.31; found: C 71.51, H 8.41, N 9.11.

**5,8,10,13,15,18-hexaamyloxy-21*H*,23*H*-tribenzo[*g*,*l*,*q*][1,2,5]thiadiazolo-[3,4-*b*]porphyrazine, $(SA_3)PzH_2$ (3a)**

*The lithium amylate method*: 1,2,5-Thiadiazole-3,4-dicarbonitrile (**1**, 1 g, 7.35 mmol) and 3,6-diamyloxyphthalodinitrile (**2**, 1 g, 3.3 mmol) were added to a solution of lithium amylate (0.28 g Li, 40 mmol) in freshly distilled amyl alcohol (30 mL). The mixture was heated under reflux for 6 h. The resulting olive-green mixture was acidified with acetic acid (5 mL) and poured into acetone (150 mL) to give a dark green precipitate which was filtered off and washed with acetone and methanol. This crude mixture of porphyrazines (1.2 g, overall yield of porphyrazines ≈60 %) was extracted with benzene in a Soxhlet apparatus. The symmetrical macrocycle $(S_4)PzH_2$ (**8a**), which is completely insoluble in benzene, remained as a solid residue (510 mg, yield ≈35 %; the UV/Vis spectrum indicates that **8a** is mixed with ≈10–15 % of $(S_3A)PzH_2$ (**6a**)). The volume of the benzene extract was reduced, and then the extract was chromatographed on aluminium oxide (Reakhim, chromatographic grade). The symmetrical amyloxy-substituted phthalocyanine $(A_4)PzH_2$ (**7a**) was eluted as the first fraction with benzene. Yield: 120 mg (3.7 %); the compound is spectroscopically identical to that obtained by direct synthesis from **2** and lithium amylate (see above), and to that reported elsewhere[47]). The second olive-green fraction containing the unsymmetrical porphyrazine **3a** was eluted with a benzene/chloroform (3:1) mixture (yield: 72 mg (2.6 %); this compound is identical to the product previously described[8] and to that obtained by the magnesium amylate method, see below). The following elution with chloroform gave the third fraction containing a mixture of the 2:2 products **4a** and **5a** and some **3a** (69 mg, ≈3 %). Elution with chloroform/acetone (9:1) gave a fourth fraction (green) containing the mixture of the 2:2 products **4a** and **5a** (96 mg, 4.1 %). The third and fourth fractions were then combined and the 2:2 species **4a** and **5a** were separated and isolated as described below in the corresponding section. The fifth bluish-green fraction containing **6a** remained on the top of the column and could not be eluted, even with pyridine. Some of this product for UV/Vis spectroscopic characterization was extracted from the alumina with boiling DMF.

*The magnesium amylate method*: Magnesium (0.2 g, 8.3 mmol) was dissolved under reflux in freshly distilled amyl alcohol (20 mL) (the reaction was initiated by addition of traces of $I_2$). 1,2,5-Thiadiazole-3,4-dicarbonitrile (**1**, 1.5 g, 11 mmol) and 3,6-diamyloxyphthalodinitrile (**2**, 1 g, 3.3 mmol) were then added and the mixture was heated under reflux (4 h). After elimination of the amyl alcohol, the residue was stirred under reflux in $CF_3COOH$ (10 mL) for 1.5 h. After the mixture had been cooled and $CF_3COOH$ had been removed by evaporation, the residue was washed with MeOH and dried. The crude material (0.87 g, overall yield ≈35 %) was extracted with $CHCl_3$ in a Soxhlet apparatus. The solvent was evaporated to give 0.68 g of a mixture of the soluble unsymmetrical porphyrazines (total yield: 27 %), and 190 mg of an undissolved solid material containing mostly the symmetrical species $(S_4)PzH_2$ (overall yield ≈10 %, calcd on the amount of **1** ≈13 %). The extract was chromatographed on silica with a $CH_2Cl_2/CHCl_3$ mixture (1:1) to give **3a** as the first fraction (70 mg, yield: 1.9 %). The second fraction was eluted with $CHCl_3$ and gave a mixture of the 2:2 products (270 mg, total yield 8.7 %), which was then treated as described below in the corresponding section. The last bluish-green fraction containing **6a** (estimated yield: 13 %) remained on the column and could not be eluted either with $CHCl_3$ containing MeOH or with DMF.

**$(SA_3)PzH_2$ (3a)**: IR (KBr): $\tilde{\nu} = 3296$ w (NH); 3058 vw $(CH)_{arom}$; 2955 m, 2927 m, 2869 m, 2858 m $(CH)_{Am}$; 1599 s, 1507 s $(CC)_{arom}$; 1466 m, 1383 m ($\delta(CH)_{Am}$); 1266 vs $(C-O)_{arom}$; 1205 s; 1123 w; 1057 s, 1012 s (O–Am); 969 w, 884 w, 797 w, 755 s, 734 m, 669 w, 639 w, 597 w, 508 m $cm^{-1}$; UV/Vis ($CH_2Cl_2$): $\lambda_{max}$ ($\log\varepsilon$) = 329(4.96), 408 sh, 458(4.29), 520 sh, 663 sh, 699 sh, 730(5.02), 766 nm (5.21); $^1H$ NMR ($CDCl_3$): $\delta = -0.25$ (s, 2H NH), 0.86 (t, $J = 6.0$ Hz, 6H, $CH_3$), 0.97 (t, $J = 7.5$ Hz, 6H, $CH_3$), 1.11 (t, $J = 7.5$ Hz, 6H, $CH_3$), 1.40–1.80 (m, 24H, $\delta$- and $\gamma$-$CH_2$), 2.21 (m, 8H, $\beta$-$CH_2$), 2.43 (m, 4H, $\beta$-$CH_2$), 4.67 (t, $J = 6.6$ Hz, 4H, $\alpha$-$CH_2$), 4.78 (t, 7.5 Hz, 4H, $\alpha$-$CH_2$), 4.82 (t, 7.2 Hz, 4H, $\alpha$-$CH_2$), 7.52 (s, 2H, CH), 7.66 (s, 2H, CH), 7.67 ppm (s, 2H, CH); FAB: *m*/*z* (%): 1039 (100) $[M]^+$; elemental analysis calcd (%) for $C_{58}H_{74}N_{10}O_6S$ (1038.55): C 67.03, H 7.18, N 13.48, S 3.08; found: C 66.70, H 7.33, N 13.47, S 2.56.

**9,12,14,17-tetraamyloxy-19*H*,21*H*-dibenzo[*l*,*q*]di[1,2,5]thiadiazolo[3,4-*b*:3,4-*g*]porphyrazine, $(S_2A_2)PzH_2$ (4a)**: 3,6-Diamyloxyphthalodinitrile (**2**, 1 g, 3.3 mmol) was added to the suspension of magnesium amylate (obtained as described above from Mg (0.2 g, 8.3 mmol) in freshly distilled amyl alcohol (20 mL)) and the mixture was heated for 10 min under reflux, followed by addition of 1,2,5-thiadiazole-3,4-dicarbonitrile (**1**, 1.5 g, 11 mmol) and reflux for further 3 h. After the mixture had been allowed to cool and the solvent had been removed by evaporation, the residue was stirred under reflux in $CF_3COOH$ (10 mL) for 1.5 h. The residue obtained after elimination of $CF_3COOH$ was washed with MeOH and dried. The crude material (0.75 g; overall yield of porphyrazines ≈30 %) was extracted with $CH_2Cl_2$ in a Soxhlet apparatus and the extract was chromatographed on alumina (grade I). The first fraction (green) was eluted with $CH_2Cl_2$ containing 1 % MeOH. After evaporation of the solvent, **4a** was obtained as a black-green powder (yield: 156 mg, 5 %). The bluish-green fraction containing **6a** remained on the top of the column and could not be eluted, even with pyridine, DMF, or acids. The solid residue

after Soxhlet extraction (370 mg) consists of the mixture of **6a** and **8a** (≈3:2, as was estimated from the UV/Vis spectrum in DMF).

**$(S_2A_2)PzH_2$ (4a)**: IR (KBr): $\tilde{\nu}$ = 3278 w (NH); 3052 vw $(CH)_{arom}$; 2954 m, 2925 m, 2867 m, 2856 m $(CH)_{Am}$; 1604 m, 1505 s $(CC)_{arom}$; 1572 w, 1543 w; 1465 m, 1384 m ($\delta(CH)_{Am}$); 1269 vs $(C-O)_{arom}$; 1209 s; 1154 m; 1123 m; 1058 s, 1030 m (O–Am); 964 w, 884 w, 799 m, 754 s, 741 m, 657 w, 623 w, 590 w, 512 w, 498 m $cm^{-1}$; UV/Vis: ($CH_2Cl_2$) $\lambda_{max}$ ($\log\varepsilon$) = 336(4.81), 514(3.97), 658(4.46), 700 sh, 735 nm (4.98); (PhMe) $\lambda_{max}$ ($\log\varepsilon$) = 333(4.72), 425 sh, 506(3.97), 657(4.48), 700 sh, 728 nm (5.06); $^1$H NMR ($CDCl_3$): $\delta$ = −1.83 (s, 2H, NH), 1.06 (t, $J$ = 7.0 Hz, 6H, $CH_3$), 1.12 (t, $J$ = 7.3 Hz, 6H, $CH_3$), 1.40–1.60 (m, 8H, $\delta$-$CH_2$), 1.69 (m, 4H, $\gamma$-$CH_2$), 1.92 (m, 4H, $\gamma$-$CH_2$), 2.14 (m, 4H, $\beta$-$CH_2$), 2.28 (m, 4H, $\beta$-$CH_2$), 4.42 (t, $J$ = 6.2 Hz, 4H, $\alpha$-$CH_2$), 4.60 (t, 7.7 Hz, 4H, $\alpha$-$CH_2$), 7.17 (d, $J$ = 8.8 Hz, 2H, CH), 7.21 ppm (d, $J$ = 8.8 Hz, 2H, CH); FAB: $m/z$ (%): 874 (100) $[M]^+$; elemental analysis calcd (%) for $C_{44}H_{50}N_{12}O_4S_2$ (875.08): C 60.39, H 5.76, N 19.21, S 7.33; found: C 60.87, H 6.15, N 19.11, S 7.23.

**5,8,14,17-tetraamyloxy-20*H*,22*H*-dibenzo[*g*,*q*]di[1,2,5]thiadiazolo[3,4-*b*:3,4-*l*]porphyrazine**, **(SASA)$PzH_2$ (5a)**: The mixture of 2:2 products (eluted with $CHCl_3$ as described above) was dissolved in $CH_2Cl_2$ and chromatographed on alumina with a $CH_2Cl_2/CHCl_3$ mixture (1:1). A continuous green band, formed upon elution, was collected in a number of fractions, which could not be differentiated by UV/Vis spectra. Only $^1$H NMR spectroscopy showed that the first eluted fraction contained the *cis* species **4a** and the terminal fraction the *trans* species **5a** of which ≈5 mg were isolated.

**(SASA)$PzH_2$ (5a)**: IR (KBr): $\tilde{\nu}$ = 3287 w (NH); 2954 m, 2923 m, 2855 m $(CH)_{Am}$; 1608 m, 1504 s $(CC)_{arom}$; 1571 w, 1540 w; 1461 m, 1386 m ($\delta(CH)_{Am}$); 1262 vs $(C-O)_{arom}$); 1204 s; 1152 m; 1119 m; 1054 m, 1035 m (O–Am); 1076 w, 1011 s, 966 w, 883 w, 801 m, 744 s, 667 s, 621 w, 606 w, 580 w, 506 m $cm^{-1}$; UV/Vis ($CH_2Cl_2$): $\lambda_{max}$ ($\log\varepsilon$) = 333 (4.80), 429 sh, 506 (3.97), 660 sh, 721 nm (4.81); $^1$H NMR ($CDCl_3$): $\delta$ = −0.87 (s, 2H, NH), 1.02 (t, $J$ = 7.0 Hz, 6H, $CH_3$), 1.13 (t, $J$ = 7.4 Hz, 6H, $CH_3$), 1.45–1.65 (m, 8H, $\delta$-$CH_2$), 1.71 (m, 4H, $\gamma$-$CH_2$), 2.01 (m, 4H, $\gamma$-$CH_2$), 2.21 (m, 4H, $\beta$-$CH_2$), 2.38 (m, 4H, $\beta$-$CH_2$), 4.57 (t, $J$ = 6.3 Hz, 4H, $\alpha$-$CH_2$), 4.72 (t, 7.0 Hz, 4H, $\alpha$-$CH_2$), 7.45 ppm (s, 4H, CH); FAB: $m/z$ (%): 874 (100) $[M]^+$.

A chromatographic procedure similar to that used to separate **5a** was used to separate **5b** from the mixture of 2:2 Mg complexes.

**[(SASA)PzMg] (5b)**: IR (KBr): $\tilde{\nu}$ = 2956 m, 2929 m, 2864 m $(CH)_{Am}$; 1610 m, 1499 s $(CC)_{arom}$; 1467 s, 1385 s ($\delta(CH)_{Am}$); 1270 vs $(C-O)_{arom}$; 1133 m; 1077 m, 1056 m (O–Am)); 504 m $cm^{-1}$; UV/Vis ($CH_2Cl_2$): $\lambda_{max}$ = 346, 455 sh, 510 sh, 650 sh, 719 nm; $^1$H NMR ($CDCl_3$): $\delta$ = 0.90 (t, $J$ = 7.0 Hz, 12H, $CH_3$), 1.39 (m, 16H, $\delta$- and $\gamma$-$CH_2$), 1.83 (qt, 8H, $\beta$-$CH_2$), 4.09 (t, $J$ = 6.4 Hz, 8H, $\alpha$-$CH_2$), 7.14 ppm (s, 4H, CH); FAB: $m/z$ (%): 898 (80) $[M+H]^+$.

**13,16-Diamyloxy-19*H*,21*H*-benzo[*q*]tri[1,2,5]thiadiazolo[3,4-*b*:3,4-*g*:3,4-*q*]porphyrazine**, **$(S_3A)PzH_2$ (6a):** 1,2,5-Thiadiazole-3,4-dicarbonitrile (**1**, 1.5 g, 11 mmol) and 3,6-diamyloxyphthalodinitrile (**2**, 0.66 g, 2.2 mmol) were added to a suspension of magnesium amylate (obtained by dissolution of Mg (0.2 g, 8.3 mmol) in freshly distilled amyl alcohol (50 mL)). The mixture was heated under reflux for 6 h, then poured into acetone (150 mL), filtered, and the solid residue was washed with acetone and methanol, and then dried. The solid was treated with hot DMF and the solution obtained was chromatographed on aluminium oxide (Reakhim, chromatographic grade). The first fraction (green) contained a mixture of the *cis* species **4b** and **5b**, the second fraction (bluish-green) contained mainly **6b**, and the third fraction (blue), containing **8b**, remained on the top of the column. The residue after extraction was washed with dilute acetic acid to remove magnesium amylate. After washing with methanol, a dark blue powder consisting mainly of **8b** admixed with **6b** was obtained. The volume of the second fraction was reduced and it was chromatographed twice to remove some admixtures of [($S_2A_2$)PzMg] and [(SASA)PzMg]. The volume of the DMF solution was reduced by distillation, the product was precipitated by pouring into hot water, centrifuged, washed with water and MeOH and then dried under vacuum to give **6b** as a DMF solvate, [($S_3A$)PzMg](DMF) (220 mg, 8.3%). For demetalation, [($S_3A$)PzMg]-(DMF) (100 mg, 0.12 mmol) was refluxed in $CF_3COOH$ and **6a** was obtained as a dark green solid after washing of residue with water and MeOH (77 mg, 90%).

**[($S_3A$)PzMg] (6b):** IR (KBr): $\tilde{\nu}$ = 2956 w, 2930 w, 2890 w, 2860 w $(CH)_{Am}$; 1646 s; 1605 s, 1500 s $(CC)_{arom}$; 1558 w, 1530 w; 1468 m, 1386 s ($\delta(CH)_{Am}$); 1308 s; 1269, 1249, 1231 s $(C-O)_{arom}$; 1153 m; 1100 s (O–Am); 1075 m, 1031 m, 969 w, 930 w, 880 m, 795 w, 771 m, 749 m, 727 m, 689 s, 677 m, 511 s, 434 w $cm^{-1}$; UV/Vis (DMF): $\lambda_{max}$ = 358, 374 sh, 628 sh, 684 nm; elemental analysis calcd (%) for [($S_3A$)PzMg](DMF), $C_{33}H_{31}MgN_{15}O_3S_3$ (806.19): C 49.16, H 3.88, N 26.06, S 11.93; found: C 48.88, H 3.97, N 26.52, S 10.92; $^1$H NMR ($C_5D_5N$): $\delta$ = 0.75 (t, 6H, $CH_3$), 1.69 (m, 4H $\delta$-$CH_2$), 2.10 (m, 4H, $\gamma$-$CH_2$), 2.39 (m, 4H, $\beta$-$CH_2$), 4.66 (t, 4H, $\alpha$-$CH_2$), 7.66 ppm (s, 2H, CH); FAB: $m/z$ (%): 733 (20) $[M-DMF]^+$.

**($S_3A$)$PzH_2$ (6a):** IR (KBr): $\tilde{\nu}$ = 3290 w (NH); 2956 m, 2924 m, 2870 w, 2852 m $(CH)_{Am}$; 1606 s, 1504 s $(CC)_{arom}$; 1576 w, 1539 m; 1464 m, 1385 s ($\delta(CH)_{Am}$); 1304 s; 1257 vs $(C-O)_{arom}$; 1203 s; 1151 m; 1117 w; 1049 s (C–OAm); 1076 w, 1012 vs, 968 w, 883 w, 806 m, 744 s, 669 m, 654 w, 606 m, 580 m, 509 s $cm^{-1}$; UV/Vis ($CH_2Cl_2$): $\lambda_{max}$ ($\log\varepsilon$) = 335 (4.83), 384 sh, 433 sh, 505 (4.19), 655 sh, 668 sh, 680 sh, 698 sh, 715 (4.80) nm.

**X-ray crystallography**: Data on $(S_2A_2)PzH_2$ and $(A_4)PzH_2$ were collected on a Brucker AXS Smart 100 CCD at 298 K with $Mo_{K\alpha}$ radiation. Solution and refinement were carried out with the programs SIR 97[48] and SHELX 93.[49]

CCDC-203249 ($(S_2A_2)PzH_2$), CCDC-203250 ($(A_4)PzH_2$) and CCDC-163159 ($(SA_3)PzH_2$[8]) contain the supplementary crystallographic data for this paper. These data can be obtained free of charge via www.ccdc.cam.ac.uk/conts/retrieving.html (or from the Cambridge Crystallographic Data Centre, 12 Union Road, Cambridge CB2 1EZ, UK; fax: (+44) 1223-336033; or e-mail: deposit@ccdc.cam.ac.uk).

**Nonlinear optical measurements**: Optical limiting measurements were carried out with 9-ns pulses at 532 nm from a doubled Nd:YAG laser (Quantel YG980E). Energies were measured with a pyroelectric detector (Scientech mod. SPHD25) by averaging 10 measurements at 2 Hz in the open-aperture configuration. Intensity of the pulses was controlled with a $\lambda/2$ wave-plate and a polarizing cube beam-splitter. Solutions were placed in 0.2-cm glass cells and the laser beam diameter on the sample was 0.3 cm with a spatial shape that resembled a top hat, as it was possible to observe with a CCD camera, and a Gaussian temporal profile. Recording of the UV/Vis spectrum of the solution makes it possible to control if a decomposition of the sample occurred. Pump and probe measurements were obtained with the same pulses used for the optical limiting measurements. A stabilized 250 W lamp, focused on the sample, was used as a probe source. The area of the probe beam was kept well within that of the pump. A Jobin–Yvon Horiba TRIAX 320 spectrometer, equipped with a 600 and a 300 groove $mm^{-1}$ gratings and a phototube (Hamamatsu R2257, rise time 2.6 ns), was used to record the probe signal. A 1 GHz digital oscilloscope (LeCroy LC564A) was used to follow the time evolution of the signal.

**Other physical measurements**: IR spectra were recorded with a Perkin-Elmer 783 spectrophotometer in the range 4000–200 $cm^{-1}$ with KBr pellets. UV/Vis spectra were obtained for $10^{-6}$–$10^{-5}$ M solutions on a Hitachi-U2000 spectrophotometer. $^1$H NMR spectra were measured on a Brucker 200 MHz Spectrometer for solutions in $CDCl_3$ or [$D_5$]pyridine. FAB experiments were carried out on a multiple quadrupole instrument (VG quattro). Elemental analyses for C, H, N, and S were provided by "Servizio di Microanalisi" at the Dipartimento di Chimica, Università "La Sapienza" (Rome) on an EA 1110 CHNS-O instrument.

## Acknowledgement

We are grateful to A. D'Arcangelo (University of Tor Vergata, Rome) for the FAB measurements, to P. Galli for elemental analyses and to M. Bassetti (Dept. of Chemistry, University of La Sapienza) for $^1$H NMR measurements. Financial support by the Ministry of Education of the Russian Federation (grant no. SPb 97-0-9.4-362) and the Italian MIUR (9903263473) is gratefully acknowledged.

[1] *Phthalocyanines: Properties and Applications*, *Vols. 1–4* (Eds.: C. C. Leznoff, A. B. P. Lever), VCH Publishers, Inc., New York, **1989–1996**.

[2] *The Porphyrin Handbook*, *Vols. 17 and 19* (Eds.: K. M. Kadish, K. M. Smith, R. Guilard), Academic Press, New York, **2003**.

[3] P. A. Stuzhin, E. M. Bauer, C. Ercolani, *Inorg. Chem.* **1998**, *37*, 1533–1539.

  

[4] E. M. Bauer, D. Cardarilli, C. Ercolani, P. A. Stuzhin, U. Russo, *Inorg. Chem.* **1999**, *38*, 6114 – 6120.
[5] E. M. Bauer, C. Ercolani, P. Galli, I. A. Popkova, P. A. Stuzhin, *J. Porphyrins Phthalocyanines* **1999**, *3*, 371 – 380.
[6] S. Angeloni, E. M. Bauer, C. Ercolani, I. A. Popkova, P. A. Stuzhin, *J. Porphyrins Phthalocyanines* **2001**, *5*, 881 – 888.
[7] C. Ercolani, E. V. Kudrik, S. Moraschi, I. A. Popkova, P. A. Stuzhin, *First International Conference on Porphyrins and Phthalocyanines* (Dijon, France) **2000**, p. 575.
[8] E. V. Kudrik, E. M. Bauer, C. Ercolani, A. Gaberkorn, P. A. Stuzhin, *Mendeleev Commun.* **2001**, 45 – 47.
[9] A paper reporting the X-ray crystal structure of a similar low-symmetry (1:3) Se-containing species, namely a $Mg^{II}$ derivative of hexapropyl(1,2,5-selenodiazolo)porphyrazine, has just appeared: S. M. Baum, A. A. Trabanco, A. G. Montalban, A. S. Micallef, C. Zhong, H. G. Meunier, K. Suhling, D. Phillips, A. J. P. White, D. J. Williams, A. G. M. Barrett, B. M. Hoffman, *J. Org. Chem.* **2003**, *68*, 1665 – 1670), following a short report with other interesting related material: M. Zhao, C. Stern, A. G. M. Barrett, B. M. Hoffman, *Angew. Chem.* **2003**, *115*, 478 – 481; *Angew. Chem. Int. Ed.* **2003**, *42*, 462 – 465).
[10] To the best of our knowledge there is only one other work which gives structural description for the series of unsymmetrical porphyrazines obtained from co-condensation of phthalodinitrile and bis(dimethylamino)maleodinitrile: A. G. Montalban, W. Jarrell, E. Riguet, Q. J. McCubbin, M. E. Anderson, A. J. P. White, D. J. Williams, A. G. M. Barrett, B. M. Hoffman, *J. Org. Chem.* **2000**, *65*, 2472 – 2478. In this work, the $Mg^{II}$ complexes of *cis*-2:2 and 3:1 species as well as metal-free 1:3 species have been characterized by single-crystal X-ray diffraction.
[11] P. A. Stuzhin, C. Ercolani in *The Porphyrin Handbook*, *Vol. 15*, *Chapt. 101* (Eds.: K. M. Kadish, K. M. Smith, R. Guilard), Academic Press, New York, **2003**, pp. 263 – 364.
[12] J. S. Shirk in *Phthalocyanines: Properties and Applications*, *Vol. 4* (Eds.: C. C. Leznoff, A. B. P. Lever), VCH Publishers, New York, **1996**, pp. 79 – 181.
[13] G. de la Torre, P. Vázques, F. Agulló-López, T. Torres, *J. Mater. Chem.* **1998**, *8*, 1671 – 1683.
[14] D. Dini, M. Barthel, M. Hanack, *Eur. J. Org. Chem.* **2001**, 3759 – 3769.
[15] S. M. O'Flaherty, S. V. Hold, M. J. Cook, T. Torres, Y. Chen, M. Hanack, W. J. Blau, *Adv. Mater.* **2003**, *15*, 19 – 32.
[16] S. R. Flom in *The Porphyrin Handbook*, *Vol. 19*, *Chapt*, *121* (Eds.: K. M. Kadish, K. M. Smith, R. Guilard), Academic Press, New York, **2003**, pp. 179 – 190.
[17] G. de la Torre, C. G. Claessens, T. Torres, *Eur. J. Org. Chem.* **2000**, *16*, 2821 – 2830.
[18] S. V. Kudrevich, N. Brasseur, C. La Madeleine, S. Gilbert, J. E. van Lier, *J. Med. Chem.* **1997**, *40*, 3897 – 3904.
[19] S. V. Kudrevich, S. Gilbert, J. E. van Lier, *J. Org. Chem.* **1996**, *61*, 5706 – 5707.
[20] M. J. Cook, A. Jafari-Fini, *J. Mater. Chem.* **1997**, *7*, 2327 – 2329.
[21] S. Sakamoto, T. Koto, M. J. Cook, *J. Porphyrins Phthalocyanines* **2001**, *5*, 742 – 750.
[22] M. J. Cook, A. Jafari-Fini, *Tetrahedron* **2000**, *56*, 4085 – 4094.
[23] T. Enokida *Jpn. Kokai Tokkyo Koho* JP 2000072975, **2000** [*Chem. Abstr*, **2000**, *132*, 209145].
[24] J. V. Bakboord, M. J. Cook, E. Hamuryudan, *J. Porphyrins Phthalocyanines* **2000**, *4*, 510 – 517.
[25] R. P. Linstead, *J. Chem. Soc.* **1953**, 2873 – 2884.
[26] C. C. Leznoff in *Phthalocyanines: Properties and Applications*, *Vol. 1* (Eds.: C. C. Leznoff, A. B. P. Lever), VCH Publishers, New York, **1989**, pp. 1 – 54.
[27] Calculations were performed with the molecular modelling package HyperChem 5.0 (Hypercube, Inc., **1997**).
[28] T. J. Hurley, M. A. Robinson, S. I. Trotz, *Inorg. Chem.* **1967**, *6*, 389 – 392.
[29] S. W. Oliver, T. D. Smith, *J. Chem. Soc. Perkin Trans. 2* **1987**, 1579 – 1582.
[30] K. J. M. Nolan, M. Hu, C. C. Leznoff, *Synlett* **1997**, 593 – 594.
[31] T. Fukuda, N. Kobayashi, *Chem. Lett.* **2002**, 866 – 867.
[32] A. Gieren, H. Betz, T. Huebner, V. Lamm, R. Neidlein, D. Droste, *Z. Naturforsch. B* **1984**, *39*, 485 – 496.
[33] I. Chambrier, M. J. Cook, M. Helliwell, A. K. Powell, *J. Chem. Soc. Chem. Commun.* **1992**, 444 – 445.
[34] I. Chambrier, M. J. Cook, P. T. Wood, *J. Chem. Soc. Chem. Commun.* **2000**, 2133 – 2134.
[35] Band assignments were made in accordance with: L. J. Bellami, *The Infra-Red Spectra of Complex Molecules*, London, Chapman and Hall, **1975**.
[36] S. M. Marcuccio, P. I. Svirskaya, S. Greenberg, A. B. P. Lever, C. C. Leznoff, K. B. Tomer, *Can. J. Chem.* **1985**, *63*, 3057 – 3069.
[37] P. A. Stuzhin, *Khim. Geterotsikl. Soedin.* **1997**, 1364 – 1370; *Chem. Heterocyclic Comp. (New York)*, (**1998**), Volume Date **1997**, *33*(10), 1185 – 1190 (Engl. Transl.).
[38] P. A. Stuzhin, O. G. Khelevina, B. D. Berezin, "Azaporphyrins: Acid – Base Properties" in *Phthalocyanines: Properties and Applications*, *Vol. 4* (Eds.: C. C. Leznoff, A. B. P. Lever), VCH Publishers, New York, **1996**, pp. 19 – 77.
[39] P. A. Stuzhin, *J. Porphyrins Phthalocyanines* **1999**, *3*, 500 – 513.
[40] P. A. Stuzhin, O. G. Khelevina, *Koord. Khim.* **1998**, *24*, 783 – 793; *Russ. J. Coord. Chem.* **1998**, *24*, 734 – 743 (Engl. Transl.).
[41] P. A. Stuzhin, E. A. Pozdysheva, O. V. Mal'chugina, I. A. Popkova, C. Ercolani, *Khim. Geterotsikl. Soedin.*, submitted.
[42] *Materials for Optical Limiting*, *Vol. 374* (Eds.: R. Crane, K. Lewis, E. Van Stryland, M. Koshnevisan), Materials Research Society, Pittsburgh, PA, **1995**.
[43] J. W. Perry, K. Mansour, I-Y. S. Lee, X.-L. Wu, P. V. Bedworth, C.-T. Chen, D. Ng, S. R. Marder, P. Miles, T. Wada, M. Tian, H. Sasabe, *Science*, **1996**, *273*, 1533 – 1536.
[44] J. S. Shirk, R. G. S. Pong, S. R. Flom, H. Heckmann, M. Hanack, *J. Phys. Chem. A*, **2000**, *104*, 1438 – 1449.
[45] W. Su, T. M. Cooper, M. C. Brant, *Chem. Mater.*, **1998**, *10*, 1212 – 1213.
[46] A. Krivokapic, H. L. Anderson, G. Bourhill, R. Ives, S. Clark, K. J. McEwan, *Adv. Mater.* **2001**, *13*, 652 – 656.
[47] M. J. Cook, A. J. Dunn, S. D. Howe, A. J. Thomson, K. J. Harrison, *J. Chem. Soc. Perkin Trans. 1*, **1988**, 2453 – 2458.
[48] A. Altomare, M. C. Burla, M. Camalli, G. Cascarano, C. Giacovazzo, A. Guagliardi, A. G. G. Moliterni, G. Polidori, R. Spagna, *J. Appl. Cryst.* **1999**, *32*, 115 – 119.
[49] G. M. Sheldrick, SHELXL 93, Program for crystal structure refinement, University of Göttingen (Germany), **1993**.

Received: March 8, 2003 [F4929]